Journal of Hydrology 569 (2019) 647–665

Contents lists available at ScienceDirect

Journal of Hydrology

journal homepage: www.elsevier.com/locate/jhydrol

Research papers

Assessment of the joint impact of extreme rainfall and storm surge on the risk of flooding in a coastal area

Bouchra Zellou*, Hassane Rahali

Institut Scientifique, University Med V, RABAT, MOROCCO, B.P.703, Rabat, Morocco

ARTICLE INFO

This manuscript was handled by Andras Bardossy, Editor-in-Chief, with the assistance of Qiuhua Liang, Associate Editor

Keywords:
Flood
Joint risk
Tide
Rainfall
Bivariate copula
Dependence

ABSTRACT

In coastal areas, flood events can result from the interaction of several factors such as rainfall, river flow and the classical tidal asymmetry to mention but a few. Therefore, flood risk assessment in these areas involves not only the estimation of the extreme values of each variable, but also their probability of occurring simultaneously. This study investigates the combined effect and dependence between a "heavy" rainfall with a high tidal levels forcing on the occurrence and severity of floods in the urban neighborhood close to the estuary of the Bouregreg River (Morocco). The methodology used for this analysis is based on a bivariate copula model to evaluate the joint risk probability of flood events. The estimated joint probability is used to define the boundary conditions for a hydraulic model to quantify the water levels and the extent of floods caused by the combination of both extreme rainfall and storm surge. The considered variables reveal a not negligible correlation, and the copula approach seems to be suitable and enough flexible, for analyzing separately marginal distributions of the source variables and their structure of dependence. Results show that the joint probability of rainfall and tide both exceeding their critical thresholds remains low to moderate, and the biggest threat to this area might be caused by heavy rainfall. However, high tide adds an extra risk by reducing the capacity of the urban drainage in absorbing storm water; especially when rainfall intensity exceeds 100 years return period. Although rainfall and tide introduce a wide range of time scale meteorological forcing, this won't prevent storm surge and extreme rainfall events resulting from climate change, to take place in the future, on the same day leading to some of the most critical flooding scenarios in this area.

1. Introduction

Estuarine hydrodynamic is controlled by the inflow of rivers, tides, the rainfall, the wind, and other oceanic events such as an upwelling, an eddy, and storms. Extreme or compound events related to all these factors, happening simultaneously or in close succession can create a situation where severe flooding may occur. This statement makes sense and is still valid even if the compound events are not all extreme per se, but only their combination (Xu et al., 2014; Lian et al., 2013; Leonard et al., 2014; Petroliagkis et al., 2016; Pappadà et al., 2017). Therefore, for more accurate assessment of flood risk in these areas, it is necessary to evaluate the dependence between these factors. There is, however, a lack of knowledge about the interaction between the hydrologic variables (rainfall, river flow, astronomical tide, storm surge…) and therefore the risk of flooding in estuarine environments is hardly quantifiable due to their dynamic nature and the complex interaction of tidal and catchment processes (Petroliagkis et al., 2016). As such, several joint probability theories have been recently incorporated into flood risk analysis including two or more hydrological variables. One of the most applied joint probability models in hydrology is the copula model. According to Sklar's theorem (1959), any multivariate joint cumulative distribution function can be expressed in terms of univariate marginal distribution functions and a copula which describes the dependence structure between the variables. The most important feature of a copula model is the way it makes it possible to model the dependence structure independently of the marginal distributions.

Therefore, many recent studies have used copula model to highlight the importance of studying the combined effect of rainfall and tide processes in estuaries and coastal areas. Lian et al. (2013) and Xu et al. (2014) investigated the joint probability and effect of the tidal level and rainfall on flood risk in a coastal city using copula-based model. They confirmed that some positive dependence exists between rainfall and tidal level, indicating that tidal level poses an additional risk of flooding. The presence of this structural and "statistical" dependence between rainfall and high tides (storm surge) has already been studied by Pugh (1987), Coles et al. (1999) and Svensson and Jones (2002) who

* Corresponding author.
E-mail address: bouchra.zellou@gmail.com (B. Zellou).

https://doi.org/10.1016/j.jhydrol.2018.12.028
Received 22 June 2018; Received in revised form 27 November 2018; Accepted 22 December 2018
Available online 27 December 2018

tried to quantify the strength of this dependence. All these studies confirmed the existence of a statistically significant dependence between extreme rainfall and extreme storm surge. Within the same spatial context, White (2009) combined traditional flood risk modeling techniques with statistical dependence to assess the relationship between river flow, tide and surge for Lewes, East Sussex, UK. He used then a one-dimensional hydraulic model to predict the joint probability of potential flood events occurring in Lewes. He concluded that a small amount of dependence between the extremes of river flow and sea level can have an important impact on the subsequent water levels in an estuary. Chen et al. (2012) established the joint distribution and calculated the coincidence probabilities of flood magnitudes and flood occurrence dates to analyze the risk of flood in the upper Yangtze River in China and the Colorado River in the United States using copula function, while Wahl et al. (2012) analyzed the statistical dependence between storm surges and wind waves in two tide stations in the German Bight using copula-based approach. Both studies confirmed that the copula concept represents a promising tool for studying multivariate problems in hydrology and coastal engineering. Similar conclusions were found by Ganguli and Reddy (2013) who used a copula-based methodology for probabilistic flood risks assessment and explored the performance of trivariate copulas in modeling dependence structure of flood properties considering peak flow, volume, and duration of flood hydrograph.

Zheng et al. (2013, 2014) studied the interaction between extreme rainfall and storm surge using bivariate logistic threshold-excess model along the Australian coastline. They reported that a significant dependence was observed for most of the tide gauge locations. Daneshkhah et al. (2016) analyzed the joint distribution of flood event properties and quantified the associated uncertainty using pair-copulas. They stated that copula is an efficient tool that can be used for probabilistic flood hazard assessment. More recently, Sebastian et al. (2017) estimated the joint exceedance probabilities for peak surge and cumulative precipitation using Bayesian network based on Gaussian copulas to model the hydraulic boundary conditions in a coastal watershed.

An issue to mention here within those studies and which has been discussed only by few authors concerns the data selected for estimating hydrological and meteorological factors' dependence. Hawkes (2008) for example, has discussed this issue and considered it as critical for dependence study. Indeed, Samuels and Burt (2002) modeled the dependence between peak river flows on the Taff at Pontypridd and sea levels at Cardiff in South Wales, UK, concluding that there was no correlation between the peak flows and the high sea levels. In contrast, a dependence analysis by Svensson and Jones (2004) for the same area found statistically significant dependence between daily mean river flow at Pontypridd and surge at Avonmouth. The contradictory conclusions may be due to the different datasets that were used, with peak river flow and peak sea level being used in Samuels and Burt (2002), and daily mean river flow and surge being used in Svensson and Jones (2004). Related to this, Zheng et al. (2013) stated that this could be because the use of peak sea level (which is in most cases dominated by astronomical tide) may lead to lower dependence compared to when using storm surge estimates directly, as it is only the latter quantity that is likely to be physically associated with extreme rainfall under the same meteorological conditions.

All these research studies have outlined the fact that univariate flood frequency analysis cannot provide a complete assessment of the occurrence probability of extremes if the underlying event is characterized by a set of interrelated random variables (Chebana and Ouarda, 2011; Masina et al., 2015). It becomes thus urgent and pressing to recognize that the risk posed by these events is likely to become more important in the future as existing coastal communities become threatened by rising sea levels and changing tidal regimes (Archetti et al., 2011; Zhang and Singh, 2007). Towns close to tidal rivers and estuaries like the ones we are dealing with in this study (Rabat and Salé, Morocco) are at risk from the combination of extreme rainfall, fluvial and tidal flooding (Egis BCEOM International/IAU-IDF/BRGM, 2011; RMSI, 2012) that can almost ruin their entire assets in the near future and set back their urban development by years or even decades. The costs of protecting these cities from rising sea levels and storms are also likely to rise with increased precipitation resulting from climate change. Furthermore, the pressure for increased urbanization of low-lying areas is expected to create major flood risk problems for many coastal and estuarine towns (Zellou and Rahali, 2017; Petroliagkis et al., 2016; Bevacqua et al., 2017).

A storm on Thursday, the 23rd of February 2017 has dumped over 120 mm of rain in just a few hours, causing flooding in the coastal neighboring cities of Rabat and Salé. The most plausible way to explain this extreme event is to account for the variability of rainfall and storm tide.

The large amounts of precipitation that fell in the surrounding area, which are normally collected by urban drainage systems and headed toward the sea or the tidal river, were partially obstructed from spilling out into the sea by the storm surge, have then contributed to major flooding along the coastal area. Ignoring therefore the storm tide's impact to flooding may necessarily lead to underestimation of the risk of flooding. This event emphasizes the importance of studying joint probabilities of extreme events and the fact that conventional univariate statistical analysis is not accurate to bring enough information regarding the multivariate nature of these events. Therefore, the present research focuses on bivariate flood frequency analysis including data preparation, parameter selection and methodology application. The source variable-pair presented here is the maximum annual 24 h rainfall and corresponding tide data. We present the application of the copula-based joint probability method to generate a combination of critical rainfall amounts and critical high tides exceeding both certain threshold values according to different return periods. Those values were applied as input to CAESAR-LISFLOOD (CL) model (Coulthard et al., 2002, 2013; Zellou and Rahali, 2017) to predict patterns of maximum water depth which may derive from different flood sources. CL model focus on the nearshore processes to replicate the tidewater hydrodynamics. Therefore, the model grid needs to be setup to include river channel, floodplain topography and nearshore bathymetry.

This study demonstrates that by putting emphasis on statistical dependence between seemingly independent variables, it is possible to investigate their multivariate extreme value distributions which are suitable for modelling the tails of multidimensional phenomena and the associated risk when these variables are above a certain critical threshold.

A parametric copula is initially fitted to the whole dataset to characterize the overall dependence structure and the tail behavior of that particular copula is extracted later. We estimate non-parametrically (Schmidt and Stadtmuller, 2006) the lower and upper tail copulas and show that the joint distribution of the rainfall and high tide level are rather upper tail dependent, a fact which cannot be detected by fitting a copula to the whole dataset. Huser et al. (2017) stated that, without firm knowledge about the tail properties of the data, it is safer (i.e., more conservative) in terms of risk of joint extremes to assume asymptotic dependence. We have proceeded, therefore, with the tails' estimation and characterization by giving a strong attention to appropriately capturing the tail extreme behavior before any joint probability evaluation. And since it is common for many environmental processes to exhibit weakening spatial dependence as events become more extreme (Huser and Wadsworth, 2018), very extreme joint risks tend to be strongly overestimated if the data exhibit decreasing dependence strength at more extreme levels (Ledford and Tawn, 1997; Davison et al., 2013). Therefore, the increase of upper tail dependence strength should be enough to explain why a copula is able to connect extreme rainfall to high tide level. The strong asymptotic dependence justification of extreme events should give evidence that concomitant extreme events are observed and both are at the same scale, and that copula provides a robust modeling framework especially when few extreme

data are available.

Here due to limited data availability, the focus of rainfall using copula is much on extreme event itself when the rainfall amount changes and implicitly not on its temporal and spatial characteristics (Müller and Kaspar, 2010; Xiao et al., 2013) in order to estimate the dependence with tide levels, since it is widely accepted that extreme precipitation changes are one type of significant perspectives to scientifically assess the behaviors and changes of climatic systems (Allan and Soden, 2008; Kysely et al., 2011; Fan et al., 2012; Li et al., 2013; Rouge et al., 2013; Xu et al., 2014). This paper takes thus, into account, only the precipitation change when we analyze its associated risk.

The paper is organized as follows: The case study area, Bouregreg estuary, is presented in Section 2. Section 3 describes the methods and the data requirements, including a brief description of copula concept and their mathematical formulation. The results of the joint risk probability of extreme rainfall and tidal levels and the consequent inundation patterns are reported and discussed in Section 4. Finally, conclusions are given in Section 5.

2. Study area

Bouregreg estuary is located in northwestern part of Morocco (Fig. 1). It belongs to an area characterized by semiarid climate with average annual rainfall of 440 mm and average annual temperature of 18 °C. The river of Bouregreg flows downstream into the Atlantic Ocean between two cities (Raba and Salé) with populations of about 577 827 and 982 163 respectively.

The close urban neighborhoods on the coastal area of Rabat and SALE have recently experienced several flood events from multiple sources (Sea and rainfall). On the night of 6 to 7 January 2014, a strong storm surge came tumbling down on the Moroccan Atlantic coast, affecting mainly the coastal zones. This phenomenon is mainly due to an atmospheric depression of the Atlantic Ocean, coupled with high winds ranging from 60 to 100 km/h northwesterly, causing giant waves of between 6 and 7 m. These extreme values can also be explained by the coincidence of high swell with a high tide up to 3–3.5 m height.

More recently, on the 23rd of February 2017, a storm dumped over 120 mm of rain in just a few hours, causing flooding in the neighboring cities of Rabat and Salé (Fig. 2). The river which normally absorbs rainwater through the sewers (urban drainage) was partially obstructed from draining into the sea by the storm surge, which then contributed to major flooding along the coast. The combined effects of high sea level and high intensity rainfall may seem to have contributed to tide-locking of drains.

The low-lying areas along these two cities' coast are susceptible to marine inundation from severe storm surge events. The major recent storm event that affected Rabat and Sale coasts occurred on February the second 2017, just 3 weeks before the flooding mentioned here above, during which a water level of 3.30 m over tide gauge zero (approximately 2.13 m above current mean sea level) was reached.

The exceptional character of this storm derived from the extremely severe meteorological contribution to the observed sea level peak; since exceptional water level continued to be recorded during the coming three weeks (3.59 m recorded the 12th of February at 03.55 AM and 3.39 at 3.20 PM; 3.52 m the 13th at 3.40AM) and must have led to the flooding of the 23rd of February 2017.

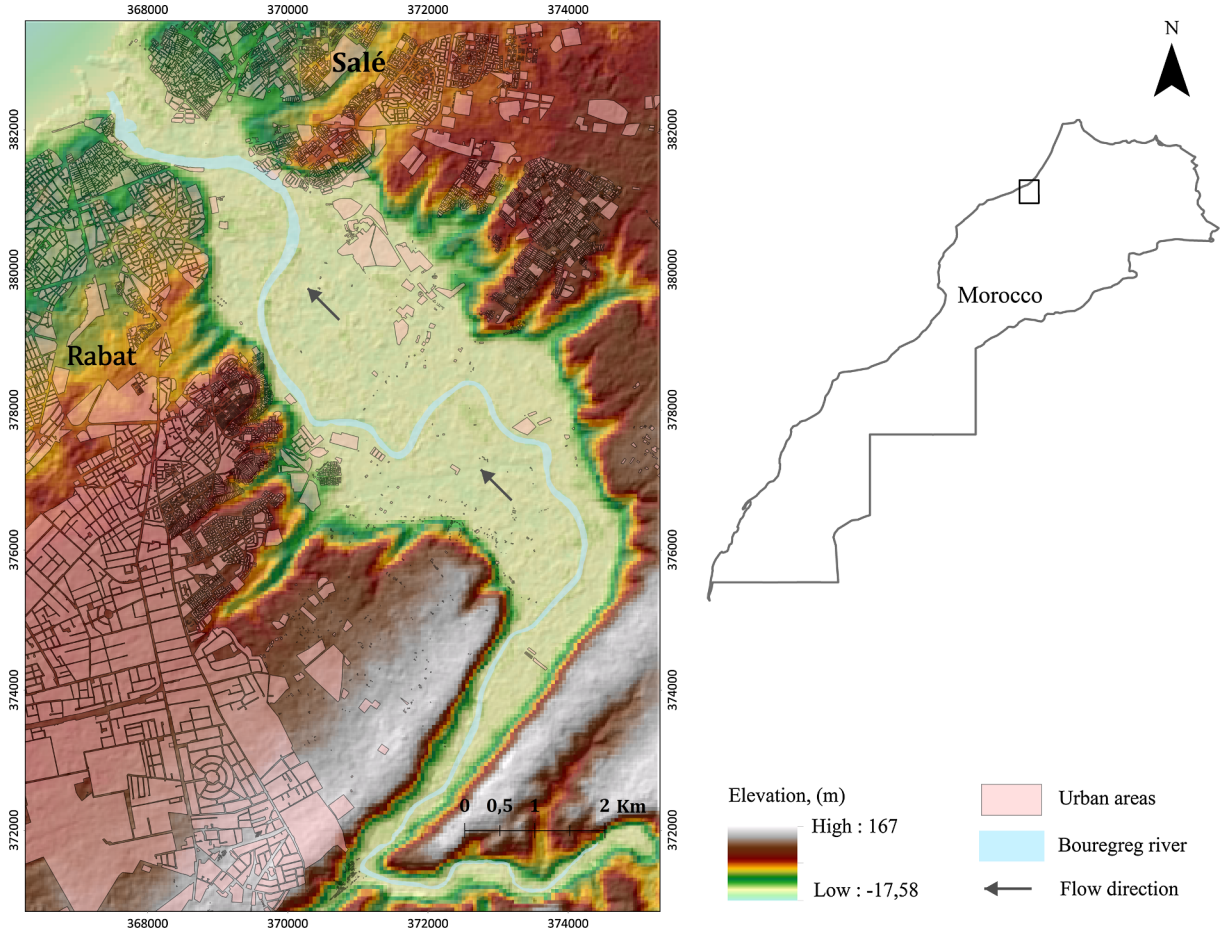

Fig. 1. Location of the study area.

Fig. 2. Flooded areas during the recent flood of the 23rd of February in the neighborhood of the two cities RABAT and SALE.

According to Jiang and Tatano (2015), focusing on urban areas, spatial flood risk assessment should reflect all risk information derived from multiple flood sources including rainfall, rivers, drainage, coast, etc., and their joint effects which may affect coastal urban areas. Therefore, an understanding of the dependence between the variables causing flood would allow a more accurate estimation of their combined probability of occurrence, thus greater confidence in the assessment and preparedness to face any associated risk.

3. Methods and data

3.1. Bivariate flood frequency analysis (Joint modelling using copula functions)

3.1.1. Copula concept

Copulas are a kind of distribution functions and have emerged as a powerful approach in simplifying multivariate stochastic Analysis (Xu et al., 2014). This method has become popular and flexible way to measure nonlinear correlation and dependencies among variables and to construct multivariate distributions. The copulas functions join multivariate distribution functions to their one-dimensional marginal distribution functions (Nelsen, 2006; Jiang and Tatano, 2015). The use of copula-based models in hydrology has gained popularity only in recent years where they were employed to estimate multivariate distribution; in the calculation of conditional probabilities and their use in bivariate simulation or in the calculation of the return periods of bivariate events (Salvadori et al., 2007; Bardossy and Pegram, 2009; Balistrocchi and Bacchi, 2011; Van den Berg et al., 2011). In this section we will present the concepts of copula theory and more precisely the Archimedean copulas. Archimedean copulas are very simple to implement thanks to the explicit relationships that link the parameter of the copula to a measure of dependence which is Kendall's tau (τ).

Let F be a 2-dimensional distribution function, with univariate margins F_1 and F_2 for random variables X and Y, respectively. According to Sklar's theorem (1959), there exists a copula C such that:

$$F(X, Y) = C(F_1(X), F_2(Y)) X, Y \in R \quad (1)$$

with C unique when $F_1(X)$and$F_2(Y)$ are continuous marginal distributions, so that

C: $[0,1]^2 \rightarrow [0,1]$ that satisfies the boundary conditions C(x,0) = C(0,x) = 0 and C(x,1) = C(1,x) = x (uniform margins) for any x∈[0,1] and the so-called 2-increasing property (Papaioannou et al., 2016). This method separates the joint distribution into a copula function and marginal distributions and has the advantage that the selection of an appropriate model for the dependence between varieties, represented by the copula, can then proceed independently from the choice of marginal distributions. As for the basic theory and concepts of copula, readers may refer to the monographs by Joe (1997) and Nelsen (2006) for additional details. For construction of high-dimensional copulas, such as nested Archimedean construction (NAC) and pair copula construction (PCC), readers may refer to Aas and Berg (2009), Savu and Trede (2010), and Czado (2010).

The Archimedean copulas are considered to be one of the well-known classes of copulas. They can capture different lower and upper tail dependencies between variables with small number of parameters because they are not restricted to radial symmetry (Hofert, 2010).

A 2-dimensional copula C is called Archimedean if it admits the representation (Nelsen, 2006):

$$C(u_1, u_2) = \psi^{-1}(\psi(u_1) + \psi(u_2)) \quad (2)$$

For some Archimedean generator ψ with its inverse function ψ^{-1}.

Fig. 3 displays the two grouped (Rainfall and Tide) data in a plot matrix. This is useful for canonical correlation analysis using Pearson's correlation coefficient (Top right panel). and regression analysis (bivariate relation) (bottom left). The top left and bottom right panels represent density plot for every variable that helps identify skewness, kurtosis and distribution information of each variable. The aim of understanding this relationship is to predict change of one variable (R) for a unit change in the other variable (T). Though, the correlation coefficient is not the only measure to conclude that 2 numeric variables are correlated even though they change with time since it is about two time series.

Although the dependence between extreme rainfall and storm surge is typically weak (Fig. 3), such weak dependence remains constant or even increases when their exceedance probabilities decrease (Zheng et al., 2014). This is referred to as asymptotic dependence and has been observed by many previous hydrological studies such as Svensson and Jones (2002), Hawkes (2008) and White (2009) to more recent analysis carried out by Zheng et al. (2013) and Lian et al. (2013). Accordingly, in this paper, we focus on the class of copulas that offer greater flexibility and allowed the modelling of complex dependence patterns and specifically for extremal dependence to able a correct estimate of the flood risk in this coastal area. While the class of elliptical copulas (Fang et al., 2002; Frahm et al., 2003) has been considered unsuitable for tail dependence analysis, the class of Archimedean copulas including Gumbel, Clayton, Frank, Joe, Ali-Mikhail Haq were considered the most flexible modeling tools when assessing the joint tail behavior of imperceptibly dependent random vectors such as rainfall and tide levels.

In this context, the five copulas from the Archimedean class (Table 1) are tested to select the best copula; the one that best fits our hydrologic data; the highest tidal level (T) during the annual maximum 24-h rainfall(R). Observations for these two random variables from 1987 to 2017 were collected as samples to estimate their joint distribution function. Depending on the joint distribution function, the joint probability of any combinations of rainfall and tidal level over some values may be assessed, including the extremes that rainfall and tidal level both exceed certain threshold values.

3.1.2. Copula selection

An important issue in using copula approach is to choose the best copula family and estimate its parameters. To select the best copula model for the pair of variables (R, T), we used the Akaike (AIC) and Bayesian Information Criteria (BIC) (Akaike, 1973; Schwarz, 1978). These criteria offer interesting advantages over frequently used statistical tests because they consider parameter dependence and they can be applied to any copula family as long as the copula density can be calculated (Silva and Lopes, 2008). That said, the AIC test is however known to have a tendency of selecting models that are too large (e.g., Claeskens and Hjort, 2008). The BIC, on the other hand, is able to consistently select the true model, but only when the number of possible parameters grows sufficiently slowly with the sample size n (Nagler et al., 2018).

For observations, $u_{i,j} i = 1, \cdots, N, j = 1, 2$ the AIC and BIC of a bivariate copula family c with parameter(s) θ are defined as:

$$AIC = -2\sum_{i=1}^{N} \ln[c(u_{i,1}, u_{i,2}|\theta)] + 2n_p \quad (3)$$

$$BIC = -2\sum_{i=1}^{N} \ln[c(u_{i,1}, u_{i,2}|\theta)] + \ln(N)n_p \quad (4)$$

where n_p is the number of parameters in the copula model ($n_p = \{1, 2\}$).

The five copulas including Gumbel, Clayton, Frank, Joe and Ali-Mikhail Haq are fitted using maximum likelihood estimation. Then the two criteria are computed for these Archimedean copulas and the family with the minimum values is selected.

3.1.3. About the joint probability and dependence strength estimation

The notion of tail dependence is more interesting in risk analysis. According to Kumar (2010), tail dependence describes the limiting proportion that one margin exceeds a certain threshold given that the other margin has already exceeded that threshold. However, like any scalar measure of dependence, tail dependence measure suffers from a certain loss of information concerning the joint behavior in the tails of the distribution. In the context of tail dependence, the immediate analogues of copulas, which describe the entire dependence structure, is given by tail copulas; refer to Schmidt and Stadtmuller (2006) and Frahm et al. (2005) for further details on tail copulas. Joe (1997) defines the tail dependence: if a bivariate copula C(u1, u2) is such that:

$$\lim_{u \to 1} \frac{[1 - 2u + C(u, u)]}{1 - u} = \lambda_U, \quad (5)$$

exists, then $C(u_1, u_2)$ has upper tail dependence for $\lambda_U \in (0, 1]$ and no upper tail dependence for $\lambda_U = 0$. This measure is extensively used in extreme value theory. It is the probability that one variable is extreme given that the other is extreme, i.e., $\lambda_U = Pr(U_1 > u|U_2 > u)$. Thus, λ_U can be viewed as a quantile-dependent measure of dependence (Coles et al., 1999).

Owing to Sklar's theorem, there exists a unique copula C for which identity, Eq. (1), holds (Genest and Favre, 2007). Therefore, just as $F_1(x)$ and $F_2(y)$ give an exhaustive description of X and Y taken separately, the joint dependence between these variables is fully and uniquely characterized by C. Nevertheless, the assessment of the dependence between variables is necessary before a copula model for a pair of variables (X, Y) is sought and before estimating joint probability of extremes. Sometimes, when dependence exists, it is more marked amongst the higher observed values (stormy conditions) than amongst the lower values. Therefore, as with single-variable extremes analysis, it can be important to choose the appropriate threshold above which to determine a dependence representative of extreme events.

Dependence checking could be done either by visualizing dependence or by the performance of statistical tests. The scatter plot of ranks, Chi-plot (Fisher and Switzer, 1985, 2001) and K-plot (Genest and Boies, 2003) are the most common graphical tools for detecting dependence; for the very reason that they are invariant with respect to monotone transformations of the variables and are thus scale free (Li et al., 2011).

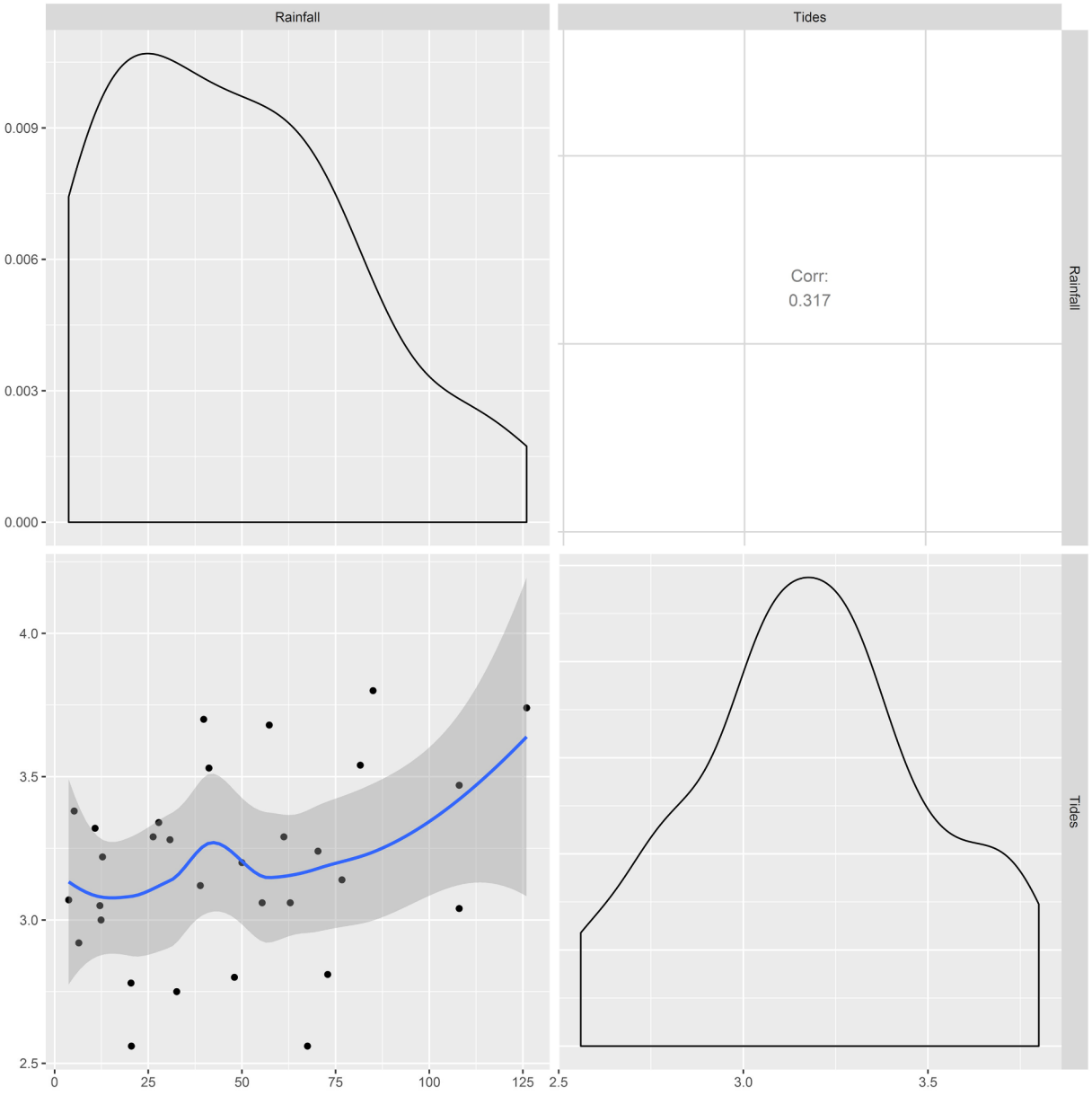

Fig. 3. Correlation between rainfall and tide data.

3.1.4. *Joint flood risk probability analysis*

Flood frequency analysis of hydrologic data consists of obtaining relationship between the magnitude of extreme events and their frequency of occurrence through the use of probability distributions (Chow, 1988; Delignette-Muller and Duttang, 2015; Ganguli and Reddy, 2013; Daneshkhah et al., 2016). In case of bivariate flood frequency analysis, the joint return period is computed using inclusive probability "AND" and "OR" (Salvadori, 2004). The first probability, in which both of the two hydrologic variables R and T exceed simultaneously their thresholds (return period), would define the boundary conditions for the hydraulic modeling of extreme joint flood events. This is the appropriate method when both variables play a role in the genesis of the risk (Eq. (6)). While the second probability "OR" assumes that only one of the parameters R or T exceeds some extreme values

Table 1
Bivariate Archimedean copulas definitions.

Copula	Generatorψ	C(u_1, u_2)	
Gumbel (1960)	$(-\ln t)^{\theta}$	$\exp\{-[(-\ln u_1)^{\theta} + (-\ln u_2)^{\theta}]^{1/\theta}\}$	$\theta \in [1, \infty)$
Clayton (1978)	$t^{-\theta} - 1$	$(u_1^{-\theta} + u_2^{-\theta} - 1)^{-1/\theta}$	$\theta \in (0, \infty)$
Frank (1979)	$-\ln\left(\frac{e^{-\theta t} - 1}{e^{-\theta} - 1}\right)$	$-\frac{1}{\theta}\ln\left[1 + \frac{(e^{-\theta u_1} - 1)(e^{-\theta u_2} - 1)}{e^{-\theta} - 1}\right]$	$\theta \in R\backslash\{0\}$
Joe (1997)	$-\ln(1 - (1 - t)^{\theta})$	$1 - [(1 - u_1)^{\theta} + (1 - u_2)^{\theta} - (1 - u_1)^{\theta}(1 - u_2)^{\theta}]^{1/\theta}$	$\theta \in [1, \infty]$
Ali, Mikhail and Haq (1978)	$\ln\left(\frac{1 - \theta(1 - t)}{t}\right)$	$\frac{u_1 u_2}{1 - \theta(1 - u_1)(1 - u_2)}$	$\theta \in [-1, \infty]$

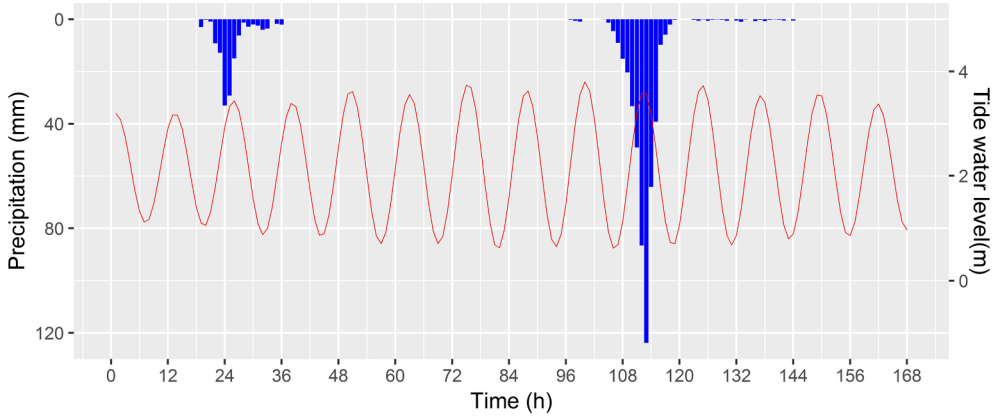

Fig. 4. The design hyetograph and the tidal curve used to simulate the 116-year joint return period event.

(Eq. (7)). This method is often used in design and safety assessment of estuary flood defenses since each of the hydrologic variable source, rainfall or tide could cause flooding (e.g. Biondi and De Luca, 2017).

The two joint exceedance probabilities are given by the following formulas:

$$P((R > r) \cap (T > t)) = 1 - F_r(r) - F_t(t) + F_c(r, t) \quad (6)$$

$$P((R > r) \cup (T > t)) = 1 - F_c(r, t) \quad (7)$$

where F_r and F_t are the distribution functions of the marginal distributions.

3.2. Hydraulic simulation of extreme joint flood event

3.2.1. Hydraulic model

CL is a geomorphological and Landscape evolution model that combines the CAESAR geomorphic model and the last version of the Lisflood-FP 2-D hydrodynamic flow model (Bates et al., 2010) to simulate erosion and depositional changes in river catchments and reaches over a range of time (from one hour to 1000's of years) and space (from 1 to 100 km) scales (Coulthard et al., 2000, 2002).

CL can be run in three modes: a catchment mode, with rainfall input; a reach mode, with points where inflow discharges are inputted to the system and a stage/tidal input mode with four coordinates delineating an area within which the tidewater levels inputs will be added to the DEM.

There are four main functions of CL, the hydrological model, slope processes, fluvial erosion and deposition, and the flow model. Only the last function will be investigated in this paper, to replicate the tidewater hydrodynamics of Bouregreg estuary in stage/tidal mode and rainfall input in catchment mode. For more detailed information about CL model equations; refer to Coulthard et al., (2000, 2002, 2013), Van de Wiel et al. (2007) and Coulthard (2011).

3.2.2. Data preparation

To simulate rainfall and tide flooding, CL requires a Digital Elevation Model (DEM) that should be set up to include not only river channel and floodplain but also nearshore bathymetry necessary to replicate the tidewater hydrodynamics. We used the Global Multi-Resolution Topography (GMRT) version 3.3 DEM (50 m pixel resolution) which brings together a variety of elevation sources delivered as multi-resolution gridded that includes land topography and ocean bathymetry (Ryan et al., 2009).

To represent spatial surface roughness, the model needs land use/cover grid file having the same format (header and extents) as the DEM. Each land use/cover class (bare ground, beach, discontinuous residential fabric, industrial area, river, road or railway space, urban green space, agricultural land, forest, sports fields, stream and urban area) is identified in the grid cell and a corresponding manning's n value is assigned to that class based on values proposed by Chow (1964).

Bed roughness controls the development of the flood wave within the CL model (lewis et al., 2013). Many studies confirmed that flood extent, water depth and velocity are also sensitive to roughness parameter (Bates and De Roo, 2000; Gallegos et al., 2009).

The manning n value that represents channel roughness can be determined based on standards proposed by Chow (1959, 1964, 1988), Barnes (1967) or Ree (1954). But due to dredging activities (man-made) and the variability of sediments rates in estuaries, this value should be well-adjusted during calibration process.

The calibration was realized using tide forcing for a year-long period (2014th) (see Fig. A.1). Four channel roughness values were tested, 0.005, 0.01, 0.015 and 0.02. These values were selected by examining the difference between simulated and observed tidewater level.

Four statistical parameters were calculated to assess model performance in predicting water level including the coefficient of determination R^2 (R-squared value), RMSE (root mean square error), MAE (Mean absolute error) and Spearman correlation.

3.2.3. Boundary conditions

The boundary conditions include the rainfall hyetograph in urban areas. Synthetic storm hyetographs and tidal input were therefore estimated based on R-T pairs generated from the fitted bivariate copula-based distribution, in order to be routed through the study area.

First, the design rainfall for different return periods (5, 10, 20 and 50 years); based on rainfall data from local Intensity-Duration-Frequency (IDF) curves (Chow, 1964) were created. A set of observed rainfall hyetograph and stage hydrograph was used as a sample to ascribe each of synthetic data shape to the chosen synthetic R-T pair via randomization achieved by coupling a stochastic rainfall generator and the hydrological model, both calibrated in the basin. Then, the resulted synthetic hyetograph for the 50-year return period was used as input to the hydraulic model CL (Fig. 4).

Tidewater level data for the Bouregreg estuary was obtained from a gauge station located at coordinates (034° 04′ 00.0″ N, 006° 46′ 00.0″ W) and using the hydrographic zero as a height reference (A 31 years of hourly tidewater level from 1987 to 2017). Optionally, when tidal station data are not available or of poor quality, CL can be driven with modelled storm surge heights applied to coastal segments with similar surge characteristics (Lewis et al., 2013; Ramirez et al., 2016).

A typical tidewater level hydrograph with one-hour time step was designed based on the results of the joint probability analysis of extreme events to run CL in tidal/stage mode (Fig. 4). This tidewater level hydrograph will be added to the nearshore location of Bouregreg River over a period of a week. By comparing the results of simulations with

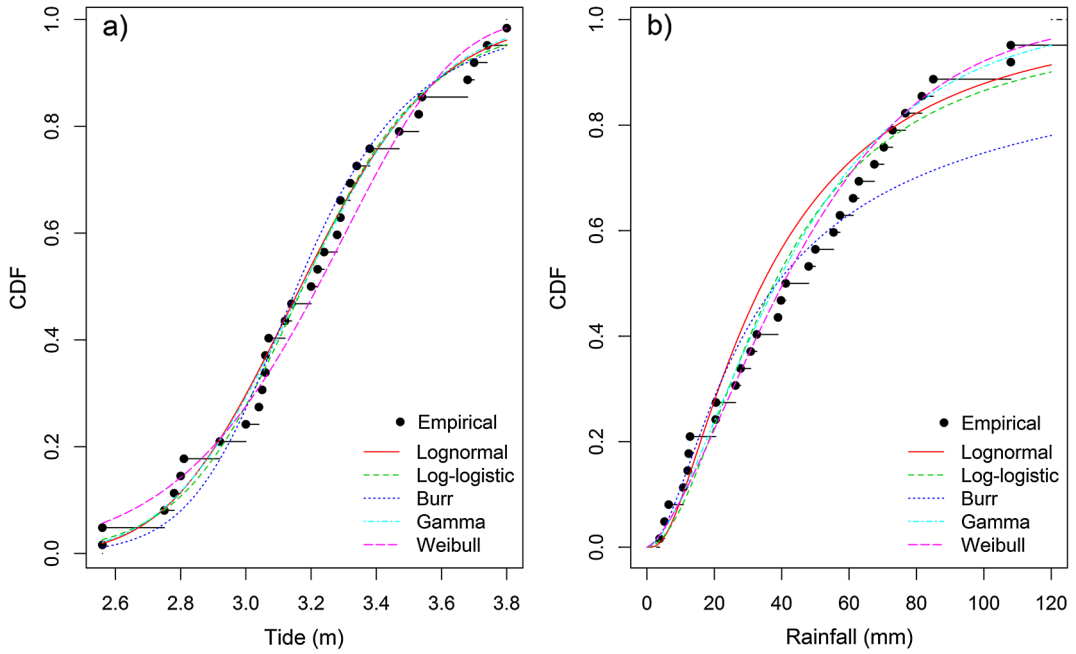

Fig. 5. Plot to compare the fit of five distributions to tide (a) and rainfall (b) data sets with Cumulative Distribution Function (CDF).

and without tide, the impact of Atlantic Ocean tide on the surface water dynamics in the Bouregreg estuary can be identified.

4. Results and discussion

4.1. Joint flood frequency analysis

4.1.1. Marginal probabilities

As stated above, one of the strong points of the copula approach is the way it makes it possible to model the dependence structure independently on the choice of the marginal laws. Therefore, the marginal distributions of the two hydrological variables [e.g. 31-year annual maximum 24-h rainfall (R) recorded at Aguibat Ezziar gauging station for the period of 1987–2017 and the highest tidal level during the annual maximum 24-h rainfall (T)] are estimated separately.

Several distributions including Burr, Lognormal, log-logistic, Gamma and Weibull were used to fit the marginal distributions of rainfall and tide data (Fig. 5).

Three goodness of fit tests; the Kolmogorov–Smirnov test (Chakravarti et al., 1967; Chowdhury et al., 1991), Cramer-von Mises and Anderson-Darling test statistics were performed to find the probabilities distribution functions that best fit Rand T. These tests were then backed up with classical penalized criteria based on the loglikelihood (AIC, BIC) to ensure that there has been no overfitting.

The purpose of these tests is to measure the distance between the fitted parametric distribution and the empirical distribution: e.g., the distance between the fitted cumulative distribution function and the empirical distribution function. Table 2 gives the definition and the empirical estimate of the three considered goodness-of-fit statistics (D'Agostino and Stephens, 1986).

Since we are interested in giving more weight to distribution's tails, the Anderson-Darling statistic is of special interest when it matters to equally emphasize the tails as well as the main body of a distribution which is often the case in risk assessment (Cullen and Frey, 1999; Vose, 2010). However, this statistic computed for several distributions fitted on the same data set are theoretically difficult to compare because the weighting of each CDF quadratic difference depends on the parametric distribution in its definition and should be moderated by looking at the result of classical penalized criteria based on the loglikelihood (AIC, BIC) to detect eventual overfitting (Delignette-Muller and Duttang, 2015).

Table 3 shows that for tide data, all the goodness-of-fit statistics based on the CDF distance are in favor of the Gamma distribution. It is the only one characterized by three parameters and confirmed by AIC and BIC values giving the preference to the Gamma distribution to be used for forecasting tides for different return periods. While the Weibull distribution adjusted using the maximum likelihood estimation (MLE) method was the most appropriate distribution for the corresponding rainfall data series. The parameters used to fit the marginal probability distributions Gamma and Weibull are shown in the Appendix (Table A.1).

Fitting a parametric distribution to data sometimes results in a model that agrees well with the data in high density regions, compared to areas of low density known as the "tails" of the distribution. One of

Table 2
Goodness-of-fit statistics as defined by D'Agostino and Stephens (1986).

Test	Formula	Computational formula
Kolmogorov-Smirnov (KS)	$sup\ \lvert Fn(x) - F(x)\rvert$	$max(D+, D-)$ *with* $D^+ = max_{i=1,\ldots,n}\left(\frac{i}{n} - F_i\right)$ $D^- = max_{i=1,\ldots,n}\left(F_i - \frac{i-1}{i}\right)$
Cramer-von Mises (CvM)	$n\int_{-\infty}^{\infty}(F_n(x) - F(x))^2 dx$	$\frac{1}{12n} + \sum_{i=1}^{n}\left(F_i - \frac{2i-1}{2n}\right)^2$
Anderson-Darl (AD)	$n\int_{-\infty}^{\infty}\frac{(F_n(x)-F(x))^2}{F(x)(1-F(x))}dx$	$-n - \frac{1}{n}\sum_{i=1}^{n}(2i-1)log(F_i(1-F_{n+1-i}))$

Table 3
Goodness of fit test statistic for distribution selection.

Goodness-of-fit statistics for tide					
	Lognormal	log-logistic	Burr	Gamma	Weibull
Kolmogorov-Smirnov	0.085	0.080	0.1	0.0798	0.10
Cramer-von Mises	0.029	0.0257	0.0485	0.0273	0.057
Anderson-Darling	0.234	0.220	0.445	0.219	0.383
AIC	22.43	23.586	27.52	22.237	23.73916
BIC	25.29	26.454	31.82	25.105	26.60714
Goodness-of-fit statistics for rainfall					
	Lognormal	log-logistic	Burr	Gamma	Weibull
Kolmogorov-Smirnov	0.134	0.113	0.211	0.0969	0.10
Cramer-von Mises	0.128	0.081	0.225	0.055	0.040
Anderson-Darling	0.773	0.655	1.47	0.349	0.279
AIC	305.68	306.46	317.90	300.97	300.11
BIC	308.54	309.33	322.20	303.84	302.98

the reasons why a model might fit poorly in the tails is that by definition, there are fewer data in the tails on which to base a choice of model, and so models are often chosen based on their ability to fit data near the mode. Add to that the fact that the distribution of real data is often more complicated than the usual parametric models. As we are primarily concerned with the identification of variables' extremal behavior, fitting the data in the tail is our main concern. The Generalized Pareto distribution (GP) has been developed as a distribution that can model tails of a wide variety of distributions, based on theoretical arguments. GP is a right-skewed distribution which is suitable for analyzing upper tail data and can be defined by construction in terms of exceedances. Starting with a probability distribution whose right tail falls to zero, like normal, we sampled 2000 random values independently of this distribution. We then fixed a threshold values for both tide and rainfall, which allows to throw out all the values that are below the threshold, and to subtract the threshold off of the values that are not thrown out, the result is known as exceedances (Fig. 6).

Fig. 6 shows the return levels with the return periods estimated on 2000 simulated sample for both rainfall and tide variables. Confidence intervals have been added to these plots as the empirical mean can be supposed to be normally distributed (central limit theorem). However,

Table 4
Extreme quantiles for R and T as a function of return period.

Return period	Maximum rainfall	Correspond tide water level
5	77.58952	3.476411
10	96.39977	3.637473
20	110.4600	3.756614
50	123.8317	3.867910

normality doesn't hold anymore for high threshold as there are less and less excesses. Table 4 gives examples of extreme quantiles estimated for four return periods.

4.1.2. Best-fit copula selection

This study applied the Archimedean class including Clayton, Frank, Gumbel, Joe and Ali-Mikhail-Haq (AMH) copulas which were tested to select the best fit copula. The parameters of each family were calculated using the maximum likelihood method (Table 5). Fig. 7 shows the scatter plots of simulated bivariate random variables based on the fitted copulas. The two criteria AIC and BIC are calculated for these copulas and the family with the smallest values is then selected. For these criteria, only the log-likelihood itself can be used to assess how well a copula model fits the data and the higher log-likelihood leads to a smaller relative AIC or BIC representing a better model fit (Killiches and Kraus, 2017). Even though, both AIC and BIC penalize the negative maximum log-likelihood of the estimated model by the number of parameters in the model (Kumar, 2010). Negative values of AIC and BIC (Table 5) can be interpreted as penalized log-likelihood functions (Joe, 2015).

As to the specific form of the dependence, no definite conclusion can be drawn. Except for Clayton, none of the other copula candidates is to be really rejected. Even the Gumbel copula could be an applicable alternative. Based on these results, the Joe copula (having the upper value of log-likelihood and lower values of AIC and BIC) is the best fit amongst the five copulas considered in this study to describe the dependence between rainfall and tide.

After copula selection, the joint bivariate distribution function was constructed taking in consideration the selected marginal distributions. Fig. 8(a) illustrates the density of the generated bivariate distribution

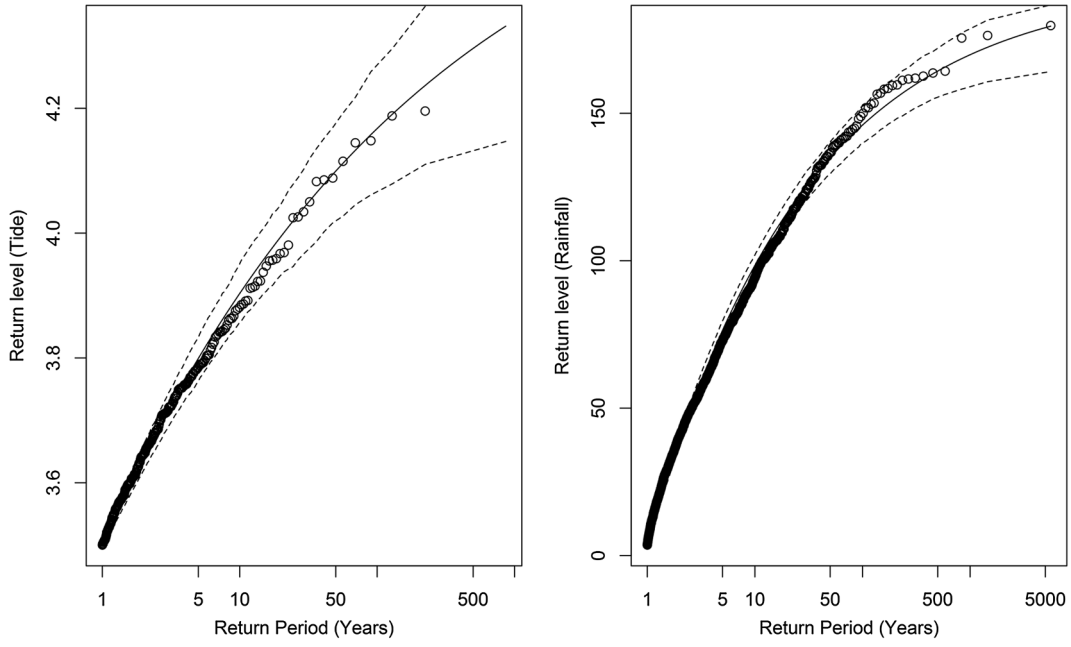

Fig. 6. GP distribution plots of tide and rainfall data with 95% confidence interval.

Table 5
Parameters and criteria selection of copula model.

Copula	Parameter θ	Kendall's tau	Log-likelihood	AIC	BIC
Gumbel	1.31	0.24	2.09	−2.18	−0.75
Clayton	0.24	0.11	0.25	1.50	2.94
Frank	1.68	0.18	1.06	−0.11	1.32
Joe	**1.54**	**0.23**	**2.65**	**−3.31**	**−1.87**
Ali-Mikhail-Haq	0.72	0.205	−0.3160815	1.367837	−0.63

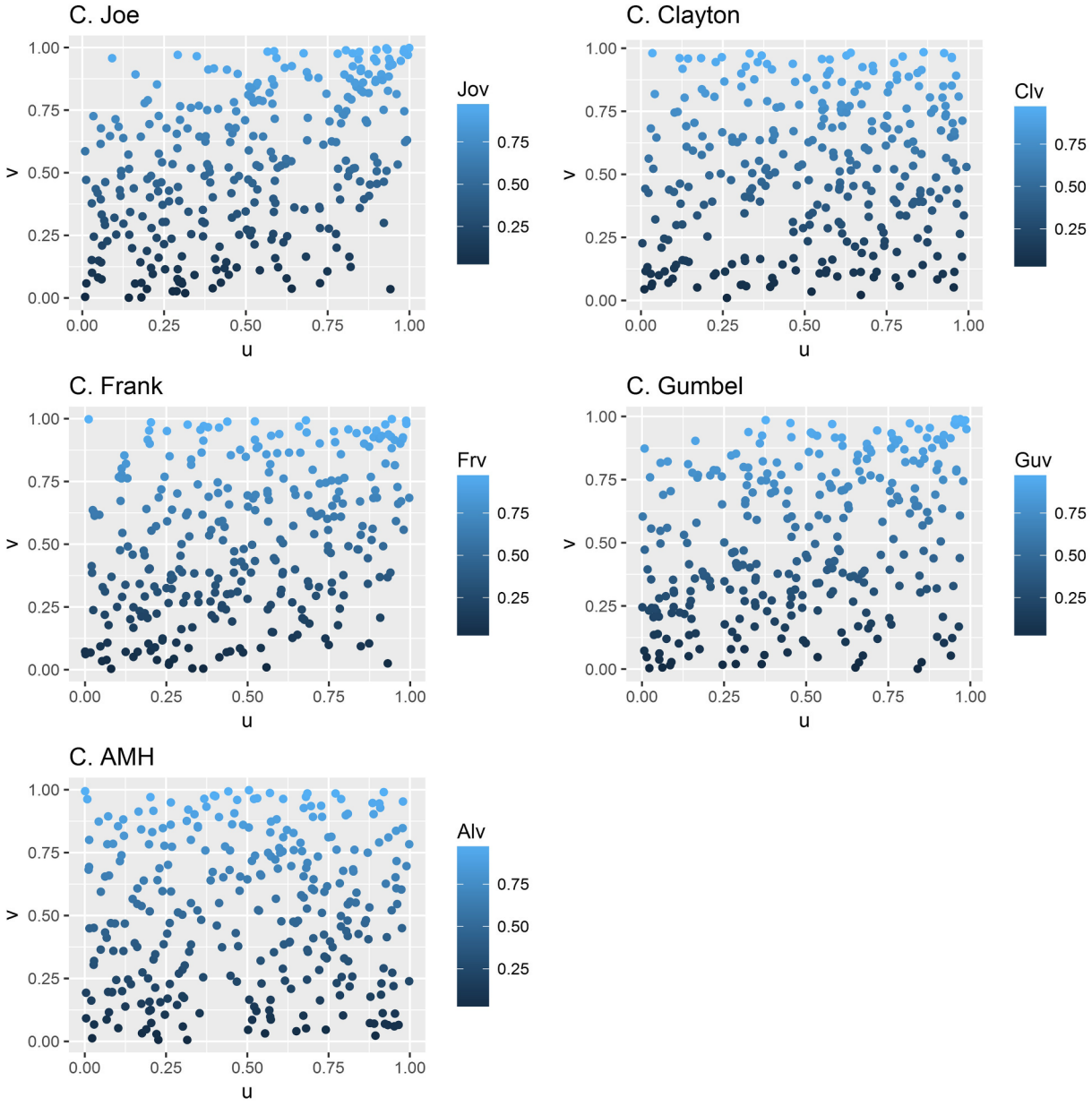

Fig. 7. Scatter plots of simulated bivariate random variables from rainfall (as the variable u along the vertical (X) axis) and tide (as the variable v along the vertical (Y) axis) marginal distributions with the five different bivariate copulas within the Archimedean class.

and Fig. 8(b) their corresponding contours and marginal distributions.

According to model selection results, the estimated joint distribution function $F_C(r, t)$ for R and T can then be presented as follows:

$$F_C(r, t) = 1 - [(1 - F_r)^{1.54} + (1 - F_t)^{1.54} - (1 - F_r)^{1.54}(1 - F_t)^{1.54}]^{1/1.54} \quad (8)$$

where F_r and F_t are Gamma and Weibull marginal distributions for maximum 24 h rainfall and tide respectively.

Fig. 8(b) shows the joint probability contours for the maximum annual rainfall and the corresponding tide levels (blue lines). To calculate the joint probability, the variables were fit to their marginal distributions and *iso*-probability contours were plotted in the probability density space. For comparison, an approximate density contour based on the empirical, bivariate data (24 h-maximum rainfall and the corresponding tide) has been drawn and added to the contour plot with colors indicating the probability density at each point (red is low

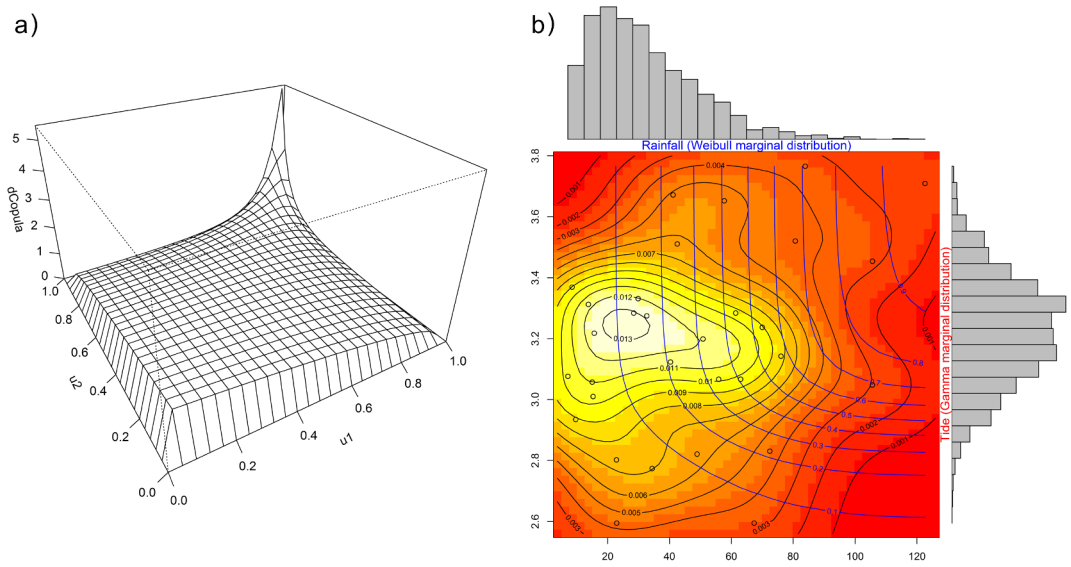

Fig. 8. (a) Density of the generated bivariate distribution using Joe copula (with u1 the uniform random variable referring to rainfall and u2 the uniform random variable referring to tide) (u1, u2 data vectors are of equal length with values in [0,1]), (b) contour lines of the joint exceedance probabilities (blue lines) calculated using Gamma and Weibull marginal distributions for the annual maximum 24 h rainfall and corresponding tide levels respectively. The points plotted in the figure represent the observed data events and contours with density (from white to red) represent an approximate density contour based on the bivariate empirical data. (For interpretation of the references to colour in this figure legend, the reader is referred to the web version of this article.)

density and white is high density). The contours in the high-density area (white) are an approximately asymmetrical ellipsis (which is what we can expect from Gamma and Weibull distributions). The density changes comparatively slowly along both rainfall and tide axes.

In practice, the interpretation of joint probabilities requires the attribution of a probability to exceed a certain threshold (th1, th2) for the two variables (rainfall and tide level) taken simultaneously. It considers thus that both variables play a role in the genesis of risk. Copula's contours (blue lines) illustrate the joint probabilities of not exceeding for both variables. From these *iso*-probability curves, we estimate the joint probabilities for different return periods as given in Table 6.

4.2. Joint flood risk probability analysis

4.2.1. Upper tail dependence analysis

In the context of extrapolation in multivariate frequency analysis, it is important to properly model the dependence of extremes, or tail dependence (Salvadori et al., 2007; Poulin et al., 2007; Frahm et al., 2005). So, before we start analyzing the joint probability, we need first to address the question whether the joint distribution of rainfall (R) and tide (T) tends to generate extreme values simultaneously and constitutes, in this sense, a dangerous combination to consider in the flood risk forecast.

To evaluate whether a copula model should be applied for the above-mentioned purpose, Kendall correlation coefficient was calculated to identify the dependence structure. The Kendall correlation coefficient was found to be 0.2325458. To visualize this dependence, we used Chi-plot and Kendall plot (Fig. 9) which represent graphically the dependence of the pair of variables (R, T).

The Chi-plot called also rank-based graphical tool is usually used in conjunction with a traditional scatterplot of the raw data. It can help detect the presence of association in a random sample from some continuous bivariate distributions. The other alternative display is the Kendall plot (K-plot for short), which adapts the concept of probability plot to the detection of dependence (Fisher and Switzer, 2001; Genest and Boies, 2003).

According to Genest and Boies (2003), K-plots are easier to interpret than chi-plots, however, because the curvature that they display in cases of association is related in a definite way to the copula characterizing the underlying dependence structure. In addition, K-plots have the advantage of being readily extendible to the multivariate context.

Fig. 9 illustrates graphically the dependence of the pair of R and T variables. As we can see, these variables are dependent; however, their dependence may be qualified as low but is still significant. According to the Chi-plot (Fig. 9(a)), the two variables seem to be independent as most of the events are found in the area between the confidence intervals (Fisher and Switzer, 1985, 2001), whereas independency on the K-plot is assumed when the events are located on the line x = y. This latter (Fig. 9(b)), provided as a complement, suggests the presence of mild positive association in the data (a positive dependence is identified if the events are located above the line, a negative dependence is indicated when the points are under the line). The conclusions obtained by the diagrams are consistent with the estimated correlation coefficients and are not so obvious from the only scatterplot (Fig. 9(c)) but in line with the empirical values of Spearman's rho (ρ) (0.2581686) and

Table 6
Joint cumulative distribution function of Joe Copula for R and T calculated for different combinations of return periods.

Copula		Correspondent tide water level in Bouregreg estuary (m)			
		3.476411	3.637473	3.756614	3.867910
Annual maximum rainfall (mm)	RP	5	10	20	50
77.58952	5	0.6949132	0.7610736	0.7861849	0.7965843
96.39977	10	0.7610736	0.8446262	0.8794234	0.8947841
110.4600	20	0.7861849	0.8794234	0.9218296	0.9424606
123.8317	50	0.7965843	0.8947841	0.9424606	0.9686554

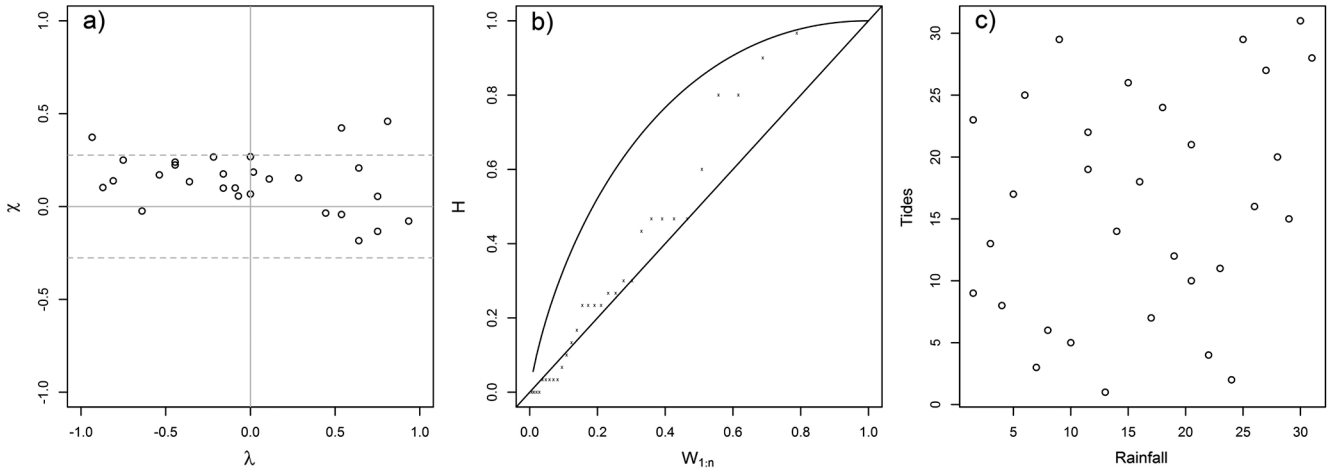

Fig. 9. (a) Kendall's plot (K-plot) (W-statistics (x-axis) and H-statistics (y-axis); H representing the ordered values of the empirical bivariate distribution function of (R, T) and $W_{i:N}$ are the expected values of the order statistics from a random sample of size N of the random variable W = C(u1,u2) under the null hypothesis of independence between u1 and u2, (b) Chi-plot for dependence analysis of rainfall and tide data (λ-statistics (x-axis) and χ-statistics (y-axis)) and (c) rank scatter plot.

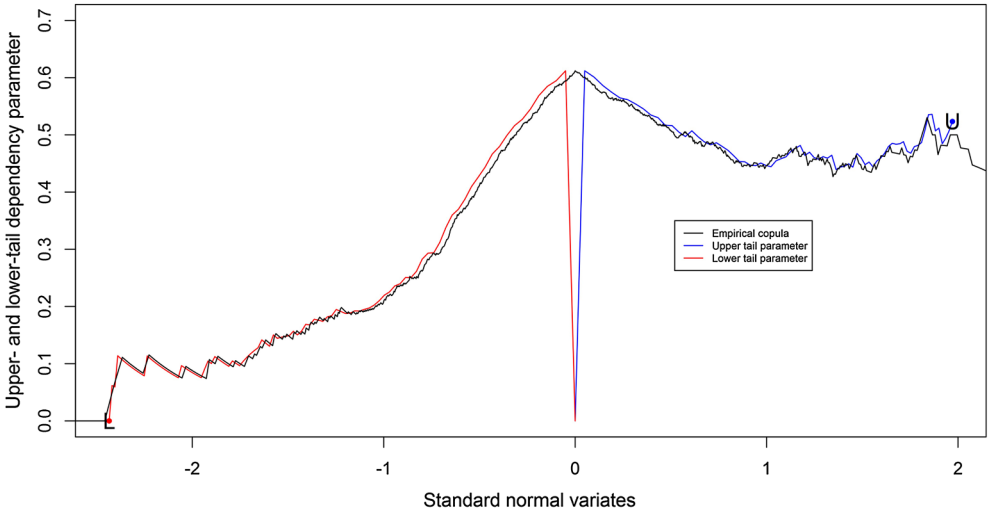

Fig. 10. Upper and lower tail dependency parameter estimation. On the y-axis, the values of λ_U and λ_L (Eqs. (9) and (10)), and on the x-axis, are values defined with reference to how much probability contained in regions near (1,1) and (0,0) (those probabilities were transformed into standard normal variates to allow the visibility of each tail).

Kendall's tau (τ) (0.23). The K-plot highlights also the presence of a cluster in the upper right corner of the rank scatter plot underlying the positive association between rainfall and tide.

It should be noted here that any scalar measure of dependence such as ρ and τ cannot describe the whole dependence structure of the joint distribution. Therefore, having concluded that R and T are positively dependent, we now address the problem of estimating their copula. In order to assess the risk of joint extreme events, we apply the concept of tail copulas. As the focus of this paper is to characterize and measure extremal dependence, the large part of this section is devoted to the concept of tail dependence, which concentrates on the upper and lower quadrant tails of the joint distribution. In the bivariate copula case, the standard way to determine whether R and T are tail dependent is to look at the so-called upper and lower tail dependence coefficients, denoted by λ_U and λ_L, respectively (Joe, 1997):

$$\lambda_U = \lim_{u\to 1} P[R > F_r^{-1}(u) | T > F_t^{-1}(u)] \quad (9)$$

$$\lambda_L = \lim_{u\to 0} P[R \le F_r^{-1}(u) | T \le F_t^{-1}(u)] \quad (10)$$

where F_r^{-1} and F_t^{-1} are the pseudo inverses of F_r and F_t respectively (F_r and F_t are the distribution functions of the marginal distributions of R and T).

Nelsen (2006) showed that tail dependence coefficients are non-parametric and depend only on the copula C and can be estimated (provided that the above limits exist (Eqs. (9) and (10)) by:

$$\lim_{u\to 1} \frac{C(1-u, 1-u)}{1-u} = \lim_{u\to 1} \frac{[1-2u+C(u,u)]}{1-u} = \lambda_U \quad (11)$$

$$\lim_{u\to 0} \frac{[C(u,u)]}{u} = \lambda_L \quad (12)$$

where: $\widetilde{C}(u_1 - u_2) = u_1 + u_2 - 1 + C(1-u_1, 1-u_2)$ is a survival copula. λ_U (Eq. (9)) is the limit of the conditional probability that R is greater than or equal to the u-th quantile of $F_r^{-1}(u)$, given that T is greater than or equal to the u-th quantile of $F_t^{-1}(u)$, and then consider the limit as u goes to 1, provided it exists. Similarly, λ_L is the limit (if it exists) of the conditional probability that R is less than or equal to the u-th quantile of $F_r^{-1}(u)$, given that T is less than or equal to the u-th quantile of $F_t^{-1}(u)$, as u approaches 0.

If $\lambda_L \in [0, 1]$, then C has lower-tail dependence but if $\lambda_L = 0$, then C has no lower-tail dependence. Likewise, if $\lambda_U = 0$, then C has no upper-tail dependence and if $\lambda_U \in [0, 1]$, then C has upper-tail dependence.

For our dataset, we found $\lambda_L = 0$ and $\lambda_U = 0.4315379$ which implies that R and T variables exhibit upper tail dependence and said to be asymptotically dependent. Therefore, large values of λ_U imply that joint extremes are more likely than for low values of λ_L. R and T might have thus a relatively strong tendency to generate extreme values simultaneously. However, the returned tail dependency values are numerically of little importance and might in strict terms be misleading. What

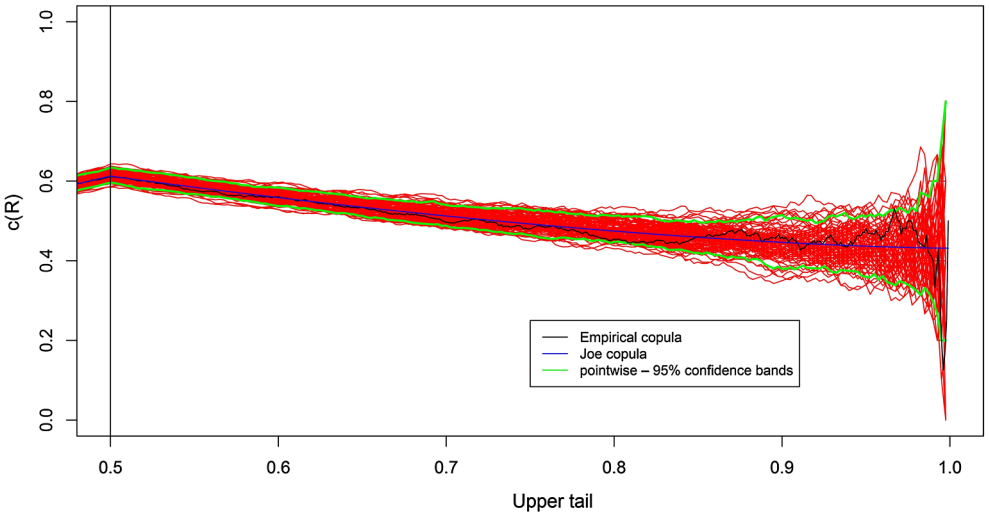

Fig. 11. Upper tail dependence fitting comparison between empirical and Joe copulas including 95% confidence interval with 100 Monte Carlo simulations. Using the tail concentration function, it is possible to see the difference in tail behaviour on probability basis between the empirical copula and Joe copula.

should be of interest is the trajectory of the lower and upper lines when plotted. Notes in (Fig. 10) how the upper tail quavers but seems to show stability towards near $\lambda_U = 0.45$ and the lower tail line varies considerably in pitch downward towards $\lambda_L = 0$.

To better visualize the limiting behavior of λ_U in which we are interested in this study, we plotted the tail dependence concentration function on the right tail according to Durante and Sempi (2015). The idea sought here is to plot, on the right, the empirical upper tail concentration function $\widehat{R}_n$ and compare it to our Joe copula tail fitting; having a Kendall's tau of 0.23 and $\theta = 1.54$ (Fig. 11).

$$\widehat{R}_n(u) = \frac{\sum_{i=1}^{n} 1(X_i > \widehat{F}_X^{-1}(u),\ Y_i > \widehat{F}_Y^{-1}(u))}{\sum_{i=1}^{n} 1(X_i > \widehat{F}_X^{-1}(u))} \tag{13}$$

The trend seen in Fig. 10 seems to be confirmed in Fig. 11. It seems also that λ_U does not exhibit the same invariance property as does copula under strictly increasing transformations of the random variables. There is, however, like for any scalar measure of dependence, a slight loss of information concerning the joint behavior in the extreme end of the distribution (Schmidt and Stadtmuller, 2006) emphasized with larger confidence interval. The statistical convergence is quite obvious underlying clearly that Joe copula has upper tail dependence.

4.2.2. Joint probability analysis

Risk analyses of natural hazards are commonly expressed as annual return periods T_r in years, which are defined for a non-exceedance probability q as $T_r = 1/(1 - q)$. Return period gives the estimated time interval between events of a similar size or magnitude. However, this definition does not state that an event of that size occurs just once inside the specified time interval but instead, it is a mean of quantifying the probability that this event will occur in any given year regardless of when the last similar event has occurred.

While in the univariate case, the return period is uniquely defined (Chow, 1988), in bivariate analysis using the best-fit copula, we can estimate probabilities of the joint behavior of R and T with some extreme values based on the joint CDF of (r, t). In this study the bivariate joint return periods called OR operator (∪) and AND operator(∩) were used (Salvadori et al., 2007; Sheng et al., 2002). There may be several combinations of R and T of which the joint probability of occurrence should be considered in flood design and mitigation. These combinations are important, as extreme flood events with extreme high rainfall and high tidewater level may cause catastrophic floods. The two inclusive risk probability events "AND" and "OR" are given in Eqs. (6) and (7). These events can be calculated based on the values ofF_r, F_t and

Table 7
Probability of simultaneously exceeding thresholds of the two variables *R*and T (The "AND" case).

P((R > r) ∩ (T > *t*))		Corresponding tide water level in Bouregreg estuary			
		3.476411	3.637473	3.756614	3.867910
Annual maximum 24 h rainfall (mm)	RP	5	10	20	50
77.58952	5	0.0949132	0.06107357	0.03618494	0.01658433
96.39977	10	0.06107357	0.0446262	0.02942336	0.01478409
110.4600	20	0.03618494	0.02942336	0.02182964	0.01246063
123.8317	50	0.01658433	0.01478409	0.01246063	0.0086554

F_C(r, t) for different combinations of return periods (Tables 7 and 8). The joint return periods corresponding to these events are then defined as:

$$T_{AND} = \frac{1}{P((R > r) \cap (T > t))} \tag{14}$$

$$T_{OR} = \frac{1}{P((R > r) \cup (T > t))} \tag{15}$$

Fig. 12 shows that as the two hazards (extreme rainfall and storm surge) can "cooperate" to cause failure for (let's say 500-year event) relative to the complement of non-exceedance joint or (inclusive) condition, the marginal probabilities must be considerably higher (up to 0.9). The green curves represent the non-exceedance joint "OR" condition. We have chosen to put the values of each variable (rainfall and tide) in their respective ranges instead of the probability scale within the interval (0, 1). Each of the lines refers to a specific return period and the values on the two axes (top and right sides are equivalent to the probabilities of occurrence of the random variables X (Rainfall) and Y (Tide) respectively; with the probability scale transformed into a Gumbel reduced variate = $-\ln(-\ln P) = -\ln[-\ln(1 - (1/RP))$; RP is the return period.

These are actually a form of level curves equivalent to an even step interval of probability such as 10-percent level curves. The complement of non-exceedance joint "OR" is the probability level that either or both random variables rainfall or tide causes "flood" at the respective return period. On the other hand, the blue curves represent the non-exceedance joint "AND" (inclusive) condition. The complement of non-exceedance joint (or inclusive) is the probability level that both random

Table 8
Probability that only one of the parameters R or T exceeds some extreme values (The "OR" case).

P((R > *fr*) ∪ (T > *t*))		Corresponding tide water level in Bouregreg estuary			
		3.476411	3.637473	3.756614	3.867910
Annual maximum 24 h rainfall (mm)	RP	5	10	20	50
77.58952	5	0.3050868	0.23892643	0.21381506	0.20341567
96.39977	10	0.23892643	0.1553738	0.12057664	0.10521591
110.4600	20	0.21381506	0.12057664	0.07817036	0.05753937
123.8317	50	0.20341567	0.10521591	0.05753937	0.0313446

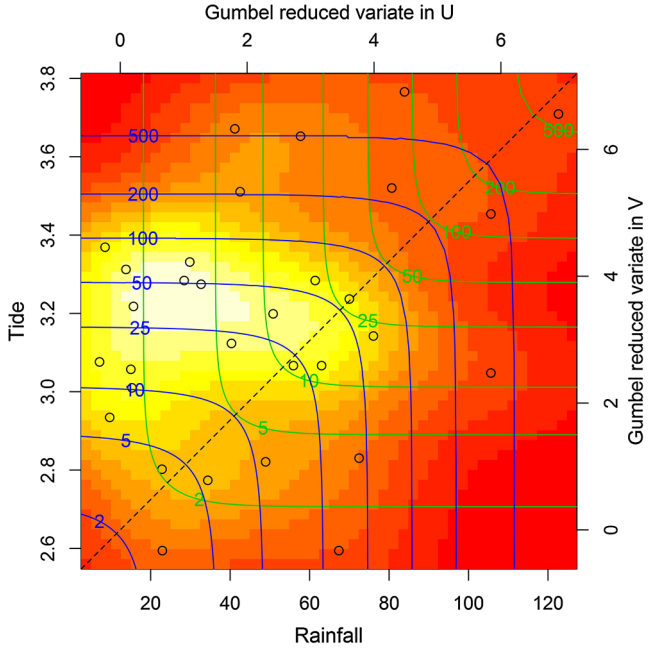

Fig. 12. Level curves for the bivariate return periods; the green curves represent the non-exceedance joint "OR" condition indicating the cooperative risk and blue curves for dual risk "AND". (For interpretation of the references to colour in this figure legend, the reader is referred to the web version of this article.)

variables (R, T) must simultaneously (or dually) occur to trigger a flooding at the respective return period. We can notice that there is obvious symmetry in the joint "OR" and "AND" curves.

Table 7 shows the probabilities of simultaneously exceeding thresholds of the two hydrological variables R and T for four marginal return periods (5, 10, 20 and 50 years). According to this table, the simultaneous occurrence probabilities of both extreme rainfall and extreme tidal level are very low. It should also be noted that this type of event is very exceptional as rainfall and tides are not governed by the same drivers, tides are mainly generated by astronomical movements of the earth, moon and sun, whereas the rainfall is principally generated by meteorological events. Dependence is more likely to exist between rainfall and the meteorological component of the tide which may both be produced by the same low-pressure weather system (Zheng et al., 2013). So, the period of thirty-one years of historical data, considered in this study, is relatively short and may not contain the rarest coincidence of extreme tide levels and rainfall, resulting in an underestimation of the intensity and occurrence of these events.

For example, the value 0.0086554, in Table 7, shows that we have 0.86% of chance per year to have an extreme rainfall exceeding 123.83 mm and tidewater level exceeding 3.86 m in the Bouregreg estuary. Thus, the joint return period associated to this event, calculated using Eq. (14), is T_{AND} = 116years while the return period associated to these quantiles in marginal distributions is 50 years (Fig. 12). This example clearly shows that neglecting a positive dependency between the maximum rainfall and the corresponding tidewater level in the studied estuary may cause an underestimation of the probability of concurrent extreme events.

The outcomes of the joint flood risk probability assessment are then used in the hydraulic modeling to determine which combination gives the highest water level at a particular location in the study area.

4.3. Flood mapping of the joint risk of extreme rainfall and tide level

4.3.1. River bed roughness calibration

River bed roughness was calibrated by comparing the predicted river and tidewater levels at different locations along the estuary with the observed data. For tidal simulation, the calibration was realized using tide forcing for a year-long period (2014th) (Fig. A.1). Four Channel roughness values were tested, 0.005, 0.01, 0.015 and 0.02.

The results of the calibration process are described in Table 9.

The closest agreement was obtained using manning's n value equal to 0.01 for low and high tide periods (Fig. 13).

The tidewater levels were correctly replicated by CL model and the results obtained agree well with the tide gauge dataset. The mean squared correlation and the mean Spearman correlation coefficients were very close to 1 (0.98 and 0.99 respectively). The RMSE values vary between 0.06 and 0.11, whereas the MAE values span from 0.05 and 0.09. Lewis et al. (2013) states that the choice of manning roughness coefficient influences tide wave propagation more than the bathymetry's uncertainty. Ramirez et al. (2016), who also used CL to simulate storm tide, concluded that the bathymetry has no effect on the storm tide and inland flooding if the storm tide has been initiated across the nearshore area. Our result also confirms this, because, despite using a DEM with a low resolution (50 m), the results of the tidal simulation appear to be good. Therefore, a good calibration process should be

Table 9
Statistical comparison of modeled water levels vs. observations for four separated weeks during the year 2014.

	RMSE (m)				MAE (m)				R^2				Spearman correlation			
	0.005	0.01	0.015	0.02	0.005	0.01	0.015	0.02	0.005	0.01	0.015	0.02	0.005	0.01	0.015	0.02
January	0.0727	0.063	0.068	0.072	0.05258	0.05252	0.056	0.059	0.9787	0.983	0.981	0.978	0.992	0.992	0.991	0.99
March	0.122	0.11	0.118	0.128	0.092	0.092	0.099	0.106	0. 980	0.984	0.981	0.978	0.990	0.992	0.991	0.989
June	0.077	0.06	0.065	0.07	0.053	0.052	0.055	0.059	0.976	0.985	0.983	0.98	0.988	0.993	0.992	0.99
November	0.108	0.101	0.107	0.114	0.085	0.086	0.09	0.096	0.981	0.983	0.981	0.979	0.989	0.991	0.99	0.989

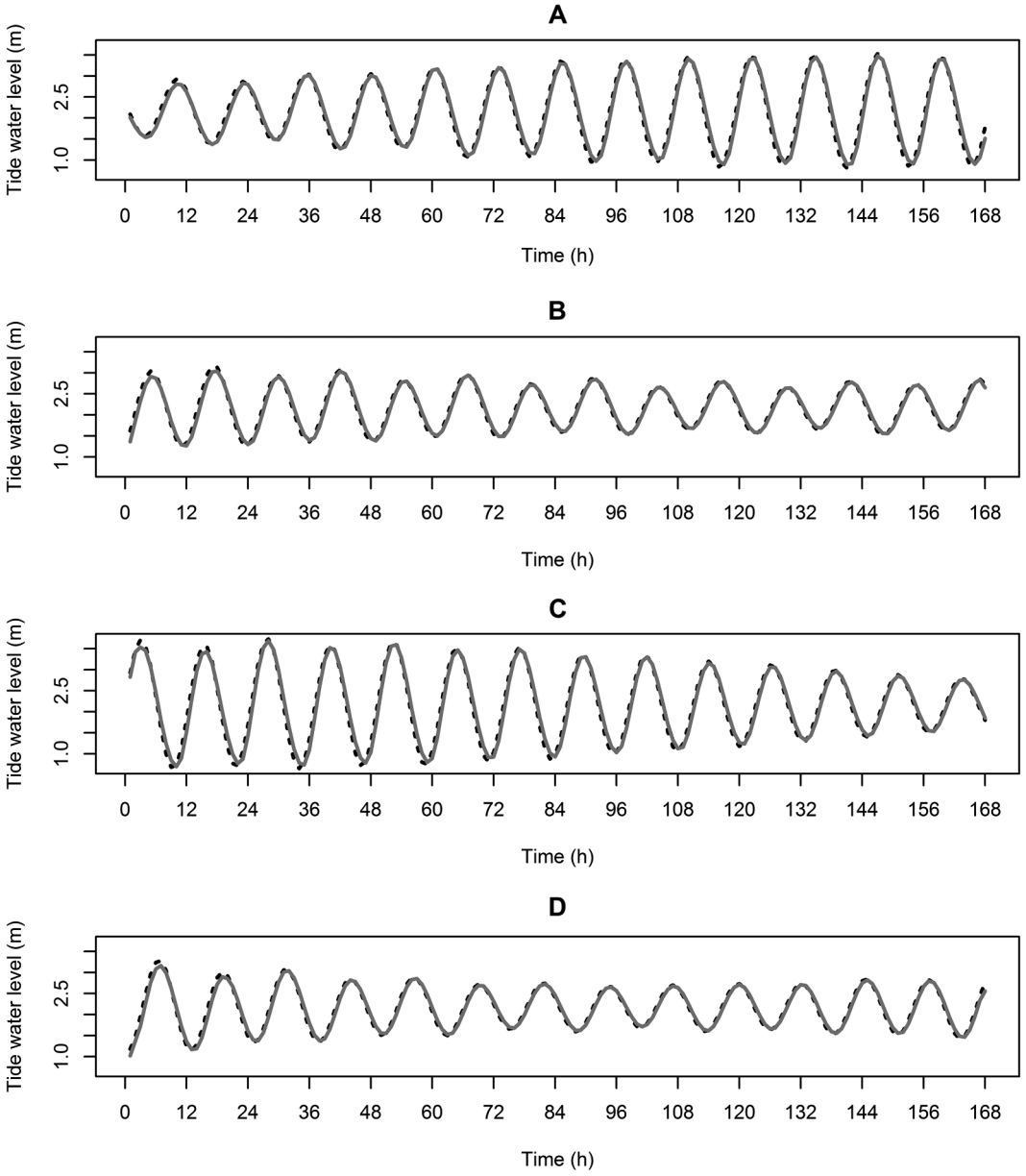

Fig. 13. Comparison between observed and simulated tidewater levels using CL model at the Bouregreg estuary for four separated weeks during the 2014th year with a bed roughness coefficient equal to 0.01. (A) from 6 to 12 January, (B) from 1 to 7 March, (C) from 1 to 7 June and (D) from 1 to 7 November. Model results are shown in solid gray line and observations in dashed black line.

applied to estimate the effect of uncertainties (lewis et al., 2013; Aronica et al., 2002; Skinner et al., 2015).

4.3.2. Flood maps

Fig. 14(A) shows maximum inundation extent and depths predicted by CL for the 116-year joint exceedance return period event using the design hyetograph and the tidal curve presented in Fig. 4. While Fig. 14(B) presents the results of the simulation using the same input design hyetograph but without tide inputs.

The 116-year joint return period flood, which is a combination of high rainfall (123.83 mm) and high tidewater level (3.87 m) generated an inundation extent similar to what has been witnessed in the coastal area and the close neighborhood during the storm of 23rd of February 2017. It is worth mentioning here that the urban network wasn't included in the simulation and that a great deal of the 23rd of February 2017 flood is to be related to the fact that rainwater which is drained through the sewers was partially or totally obstructed from pouring into the sea. The combined effects of high sea level and high intensity rainfall seem to have contributed to tide-locking of urban drains and the rise of water level in the river channel and its floodplain in the estuarine area. The accumulation of runoff water from the two cities, which is supposed to be absorbed by the river and released into the ocean, has been blocked by tidal currents producing an increase in the water level around the river mouth and then the propagation of flood to the inland region. The spread of the ocean tide to the inland area is thus highly regulated by the spatiotemporal distributions of the absolute water surface elevations (Yamazaki et al., 2012).

There is no other plausible way than the multivariate analysis using the concept of copula, to explain this rare event which caused the interruption of road and rail traffic between the North and South of the country for several hours. Furthermore, the rapid growth of urbanization combined with the impacts of climate change, along with the sea-level rise and the frequency and severity of rainfall can only worsen the risk of flooding. In view of this, the univariate flood frequency analysis

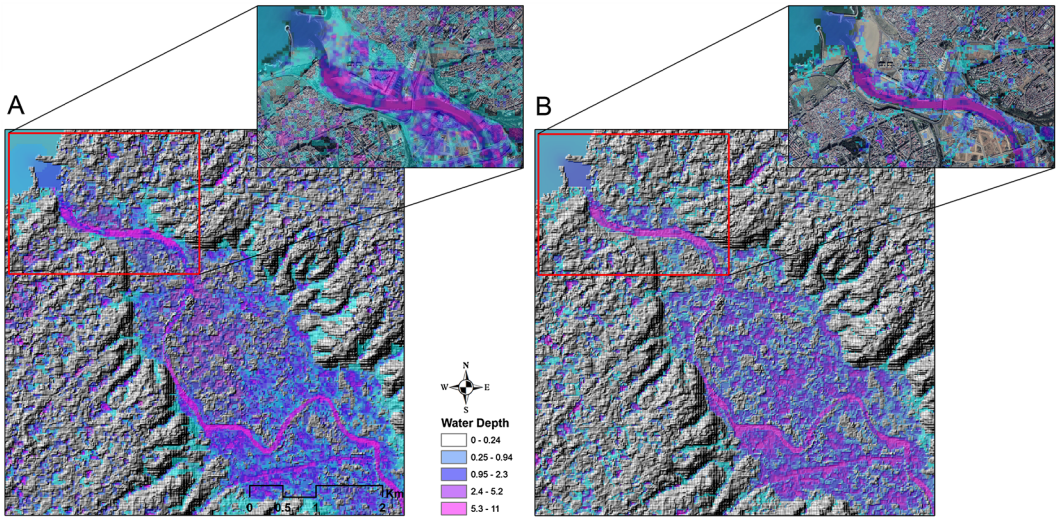

Fig. 14. Inundation extent and water depths predicted by CL after a week of rainfall scenario A: with tide inputs and B: without tide inputs.

seems to be insufficient to design flood Risk plan and mitigation. Despite the fact that the joint probability method is still considered a research topic and is not widely used in flood risk management plans (Hawkes, 2005), it would be highly recommended in the case in point; especially that the site is undergoing a big urban structuring project. The area will undergo profound changes with a high density of habitats by 2030. This significant urban extension will increase the stakes related to flood management on a site highly exposed to the risks of flooding and marine submersion if all flood's inducing factors are not considered.

5. Conclusion

In this paper, the joint impact of extreme rainfall and extreme tide level on flood risk is assessed in Bouregreg estuary, including the joint flood risk probability analysis using bivariate copula model.

The joint probability method consists, basically, on the choice of the marginal law of each hydrological variable separately. The Weibull and the Gamma distributions adjusted using the maximum likelihood method were the most appropriate distributions for the rainfall and the corresponding tidewater level series, respectively. The second step involves the selection of the copula that best fit our hydrologic data. Five Archimedean copulas including Gumbel, Clayton, Joe, Frank and Ali Mikhael Haq are compared using the two criteria AIC and BIC. The Joe copula is chosen as the best fit copula and it is then used to model the joint cumulative distribution function of the flood variables in this study. The bivariate dependence structure was then checked using many rank-based graphical tools like the scatter plot of ranks, Chi-plot and Kendall plot. The results of these dependence measures and the analysis of tail dependence coefficients confirmed that a significant dependence exists between these two hydrological variables. Even in cases where the dependence was low, the correlation between rainfall and tide was still not negligible. Finally, the joint return periods of flood using this copula are computed, analyzed and then used to define the boundary conditions for the hydraulic modeling of extreme joint flood events.

Based on the joint flood risk probability analysis, the simultaneous occurrence probabilities of both extreme rainfall and extreme tidal level are very low; this can be explained by the short duration of the hydrologic input series which may not contain these rare events. However, hydraulic simulations of these low frequency flood events, which consist of rainfall input combined with high water levels from an exceptional tide in the Bouregreg estuary, show that ignoring the dependence between these hydrologic variables may lead to considerable underestimation of both the maximum flood water levels and extension. Flooding can occur whenever a significant amount of precipitation falls in only few hours. The risk increases if this rainfall coincides with high tide or if the ground is already saturated by consecutive days of precipitation.

The comparison of simulated and recorded tide height showed that the tidal fluctuations were accurately simulated by the hydraulic model which has proved to be a valuable tool for simulating both tidal and fluvial hydrodynamics in data-poor regions. The analysis of the compound flood event (rainfall, tide) show that, during high tides, water from the Atlantic Ocean pushes inland into inlets, causing water levels throughout the region to rise. The runoff water accumulated from the two cities, which is supposed to be absorbed by the river and released into the ocean is then blocked and backflow into the inland area.

This study allowed understanding the spatial evolution of flooding, caused by the combination of high rainfall and high tide level, and hence identifying flood-prone areas for these low-frequency and high-risk flood events. It could also provide a significant support for flooding preparedness in the Bouregreg estuary, taking into account that, design measures adequate for more than 10 years return period would not be sufficient any more in the near future.

Declaration of interest statement

The authors whose names are cited here above have participated in (a) conception and design, or analysis and interpretation of the data; (b) drafting the article or revising it critically for important intellectual content; and (c) approval of the final version.

This manuscript has not been submitted to, nor is under review at, another journal or other publishing venue.

The authors have no affiliation with any organization with a direct or indirect financial interest in the subject matter discussed in the manuscript.

Acknowledgments

We would like to thank the editor and the three anonymous reviewers for their constructive comments, which helped us to improve the manuscript.

This study was funded by a CNRST (National Centre for Scientific and Technical Research (Morocco)) excellence doctoral research grant (J01/054UM5A2014).

Appendix

Table A1
The probability density functions (PDFs) of marginal distributions (Gamma for tide and Weibull for rainfall) and their associated parameters.

Marginal distribution	Probability Density Function (PDF)	Parameters
Gamma	$f_X(x) = \frac{\alpha^\beta x^{\beta-1} e^{-\alpha x}}{\Gamma(\beta)}$; $x \geq 0$, α, $\beta > 0$;	Scale parameter : α = 29.99
	CDF defined as: $\Gamma(\beta) = \int_0^\infty t^{\beta-1} e^{-t} dt for \beta > 0$	Shape parameter β = 95.53
Weibull	$f_X(x) = \frac{\beta}{\alpha}\left(\frac{x}{\alpha}\right)^{\beta-1} e\left[-\left(\frac{x}{\alpha}\right)^\beta\right]$	Scale parameter: α = 52.22 Shape parameter β = 1.435346

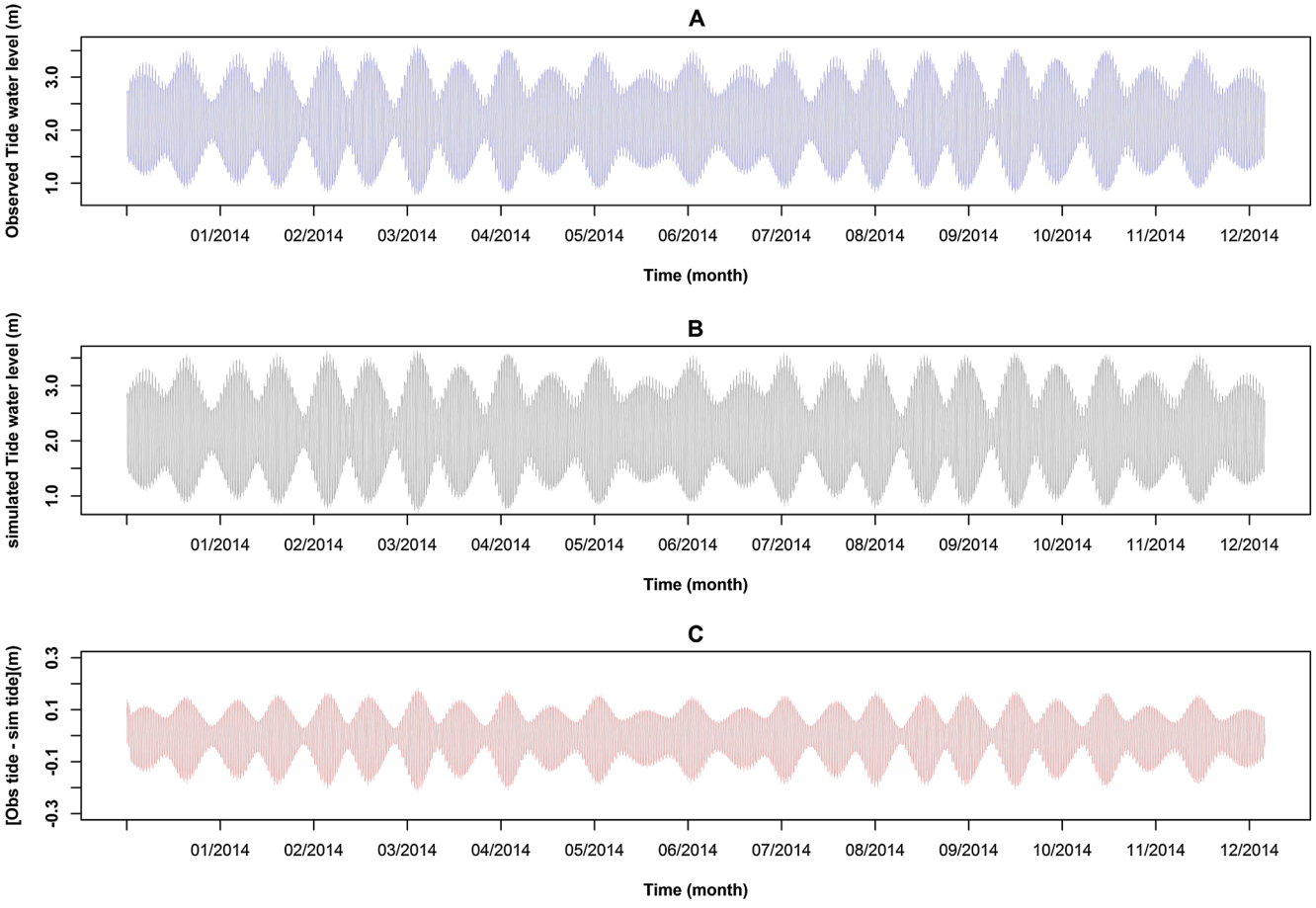

Fig. A.1. Tidal simulation for a year-long period (2014th). (A) Observed tidewater level during 2014, (B) simulated tidewater level using CL, (C) difference between simulated and observed tidewater level.

References

Aas, K., Berg, D., 2009. Models for construction of multivariate dependence – a comparison study. Eur. J. Finance 15, 639–659 10.1080/13518470802588767.

Akaike, H., 1973. Information theory and an extension of the maximum likelihood principle. In: Petrov, B.N., Csaki, F. (Eds.), Proceedings of the Second International Symposium on Information Theory Budapest. Akademiai Kiado, pp. 267–281.

Ali, M.M., Mikhail, N.N., Haq, M.S., 1978. A class of bivariate distributions including the bivariate logistic. J. Multivariate Anal. 8, 405–412. https://doi.org/10.1016/0047-259X(78)90063-5.

Allan, R.P., Soden, B.J., 2008. Atmospheric warming and the amplification of precipitation extremes. Science 321 (5895), 1481–1484.

Archetti, R., Bolognesi, A., Casadio, A., Maglionico, M., 2011. Development of flood probability charts for urban drainage network in coastal areas through a simplified joint assessment approach. Hydrol. Earth Syst. Sci. 15, 3115–3122. https://doi.org/10.5194/hess-15-3115-2011.

Aronica, G., Bates, P.D., Horritt, M.S., 2002. Assessing the uncertainty in distributed model predictions using observed binary information within GLUE. Hydrol. Processes 16, 2001–2016.

Balistrocchi, M., Bacchi, B., 2011. Modelling the statistical dependence of rainfall event variables through copula functions – Hydrol Earth Sys. Science 15 (6), 1959–1977.

Barnes, H.H., 1967. Roughness characteristics of natural channels: U.S. Geological Survey Water-Supply Paper 1849, 213 p.

Bardossy, A., Pegram, G.G.S., 2009. Copula-based multisite model for daily precipitation simulation. Hydrol. Earth Syst. Sci. 13 (12), 2299–2314.

Bates, P.D., De Roo, A.P.J., 2000. A simple raster-based model for flood inundation simulation. J. Hydrol. 236, 54e77. https://doi.org/10.1016/S0022-1694(00)00278-X.

Bates, P.D., Horritt, M.S., Fewtrell, T.J., 2010. A simple inertial formulation of the shallow water equations for efficient two-dimensional flood inundation modeling. J. Hydrol. 387 (1–2), 33–45. https://doi.org/10.1016/j.jhydrol.2010.03.027.

Bevacqua, E., Maraun, D., Hobæk Haff, I., Widmann, M., Vrac, M., 2017. Multivariate

statistical modelling of compound events via pair-copula constructions: analysis of floods in Ravenna (Italy). Hydrol. Earth Syst. Sci. 21, 2701–2723. https://doi.org/10.5194/hess-21-2701-2017.
Biondi, D., De Luca, D.L., 2017. Rainfall-runoff model parameter conditioning on regional hydrological signatures: application to ungauged basins in southern Italy. Hydrol. Res. 48, 714–725. https://doi.org/10.2166/nh.2016.097.
Chakravarti, I.M., Laha, R.G., Roy, J., 1967. Handbook of Methods of Applied Statistics, Vol I, 392–394.
Chebana, F., Ouarda, T., 2011. Multivariate quantiles in hydrological frequency analysis. Environmetrics 22, 63–78. https://doi.org/10.1002/env.1027.
Chen, L., Singh, V.P., Shenglian, G., Hao, Z., Li, T., 2012. Flood coincidence risk analysis using multivariate copula functions. J. Hydrol. Eng. 17, 742–755. https://doi.org/10.1061/(ASCE)HE.1943-5584.0000504.
Chow, V.T., 1959. Open-channel hydraulics. McGraw- Hill Book Company, New York, pp. 680.
Chow, V.T., 1964. In: Handbook of Applied Hydrology. McGraw-Hill Book Company, pp. 1–1450.
Chow, V.T., 1988. Open-Channel Hydraulics. McGraw-Hill, New York (NY).
Chowdhury, J.U., Stedinger, J.R., Lu, L., 1991. Goodness-of-fit tests for regional generalized extreme value flood distributions. Water Resour. Res. 27 (7), 1765–1776.
Clayton, D.G., 1978. A model for association in bivariate life tables chronic disease incidence. Biometrika 65 (1), 141–151. https://doi.org/10.1093/biomet/65.1.141.
Claeskens, G., Hjort, N., 2008. In: Model Selection and Model Averaging. Cambridge University Press, Cambridge. https://doi.org/10.1017/CBO9780511790485.
Coles, S., Heffernan, J., Tawn, J., 1999. Dependence measures for extreme value analyses. Extremes 2 (4), 339–365.
Coulthard, T.J., 2011. The CAESAR model. University of Hull, UK. http://www.Coulthard.org.uk/CAESAR.html.
Coulthard, T.J., Kirkby, M.J., Macklin, M.G., 2000. Modelling geomorphic response to environmental change in an upland catchment. In: Hydrological Processes, Special Issue: Geocomputation in Hydrology and Geomorphology. Wiley & Sons, UK, pp. 2031–2045 11–12.
Coulthard, T.J., Macklin, M.G., Kirkby, M.J., 2002. A cellular model of Holocene upland river basin and alluvial fan evolution. Earth Surf. Processes Landforms 27 (3), 269–288. https://doi.org/10.1002/esp.318.
Coulthard, T.J., Neal, J.C., Bates, P.D., Ramirez, J., de Almeida, G.A.M., Hancock, G.R., 2013. Integrating the LISFLOOD-FP 2-D hydrodynamic model with the CAESAR model: implications for modelling landscape evolution. Earth Surface Processes and Landforms n/a–n/a. https://doi.org/10.1002/esp.3478.
Cullen, A.C., Frey, H.C., 1999. Probabilistic Techniques in Exposure Assessment, 1st edition. Plenum Publishing Co.
Czado, C., 2010. Pair-Copula Constructions of Multivariate Copulas. In: Jaworski, P., Durante, F., Härdle, W.K., Rychlik, T. (Eds.), Copula Theory and Its Applications. Springer, Berlin Heidelberg, Berlin, Heidelberg, pp. 93–109.
D'Agostino, R.B., Stephens, M.A., 1986. Goodness-of-Fit Techniques, 1st edition. Dekker.
Daneshkhah, A., Remesan, R., Chatrabgoun, O., Holman, I.P., 2016. Probabilistic modeling of flood characterizations with parametric and minimum information pair-copula model. J. Hydrol. 540, 469–487. https://doi.org/10.1016/j.jhydrol.2016.06.044.
Davison, A.C., Huser, R., Thibaud, E., 2013. Geostatistics of dependent and asymptotically independent extremes. Math. Geosci. 45, 511–529.
Delignette-Muller, M.L., Duttang, G., 2015. fitdistrplus: An R Package for Fitting Distributions. J. Stat. Software 64 (4).
Durante, F., Sempi, C., 2015. Principles of copula theory: Boca. CRC Press, Raton, pp. 315.
Egis BCEOM International/IAU-IDF/BRGM., 2011. Phase 1: Évaluation des risques en situation actuelle et à l'horizon 2030 pour la vallée du Bouregreg [Risk Assessment for the Present Situation and Horizon 2030 for Bouregreg Valley]. A. Bigio, World Bank. French.
Fan, X., Wang, Q., Wang, M., 2012. Changes in temperature and precipitation extremes during 1959–2008 in Shanxi, China. Theor Appl Climatol 109 (1–2), 283–303.
Fang, H.B., Fang, K.T., Kotz, S., 2002. The meta-elliptical distributions with given marginals. J. Multivariate Anal. 82, 1–16 Corrigendum: Journal of Multivariate Analysis 94, 222–223.
Fisher, N.I., Switzer, P., 1985. Chi-plots for assessing dependence. Biometrika 72, 253–265. https://doi.org/10.1093/biomet/72.2.253.
Fisher, N.I., Switzer, P., 2001. Graphical assessment of dependence: is a picture worth 100 tests? Am. Statistician 55, 233–239. https://doi.org/10.1198/000313001317098248.
Frahm, G., Junker, M., Szimayer, A., 2003. Elliptical copulas: applicability and limitations. Statist. Probab. Lett. 63, 275–286.
Frahm, G., Junker, M., Schmidt, R., 2005. Estimating the tail dependence coefficient. Insurance: Math. Econ. 37, 80–100.
Frank, M.J., 1979. On the simultaneous associativity of F(x, y) and x + y-F(x, y). Aequationes Mathematicae 19 (1), 194–226. https://doi.org/10.1007/BF02189866.
Gallegos, H.A., Schubert, J.E., Sanders, B.F., 2009. Twodimensional, high-resolution modeling of urban dam-break flooding: a case study of Baldwin Hills California. Adv. Water Resour. 32, 1323–1335.
Ganguli, P., Reddy, M.J., 2013. Probabilistic assessment of flood risks using trivariate copulas. Theor. Appl. Climatol. 111, 341. https://doi.org/10.1007/s00704-012-0664-4.
Genest, C., Boies, J.-C., 2003. Detecting Dependence with Kendall Plots. Am. Statistician 57, 275–284.
Genest, C., Favre, A.-C., 2007. Everything you always wanted to know about copula modeling but were afraid to ask. J. Hydrol. Eng. 12, 347–368 10.1061/(ASCE)1084-0699(2007) 12:4(347).
Gumbel, E.J., 1960. Bivariate exponential distributions. J. Am. Stati. Assoc. 55, 698–707.
Hawkes, P.J., 2005. Use of Joint Probability Methods in Flood Management, A Guide to Best Practice R&D Technical Report FD2308/TR2. Defra/Environment Agency Flood and Coastal Defence R&D Programme.
Hawkes, P.J., 2008. Joint probability analysis for estimation of extremes. J. Hydraul. Res. 46, 246–256.
Hofert, M., 2010. Construction and Sampling of Nested Archimedean Copulas. In: Jaworski, P., Durante, F., Härdle, W., Rychlik, T. (Eds.), Copula Theory and Its Applications. Lecture Notes in Statistics. Springer, Berlin, Heidelberg.
Huser, R., Opitz, T., Thibaud, E., 2017. Bridging asymptotic independence and dependence in spatial extremes using Gaussian scale mixtures. Spatial Statistics 21, 166–186. https://doi.org/10.1016/j.spasta.2017.06.004.
Huser, R., Wadsworth, J.L., 2018. Modeling spatial processes with unknown extremal dependence class. J. Am. Stat. Assoc. 1–11. https://doi.org/10.1080/01621459.2017.1411813. Theory and Methods.
Jiang, X., Tatano, H., 2015. A rainfall design method for spatial flood risk assessment: considering multiple flood sources. Hydrol. Earth Syst. Sci. Discuss. 12, 8005–8033. https://doi.org/10.5194/hessd-12-8005-2015.
Joe, H., 1997. Multivariate Models and Multivariate Dependence Concepts, Chapman & Hall/CRC Monographs on Statistics & Applied Probability. Taylor & Francis.
Joe, H., 2015. Dependence Modeling with Copulas. Monographs on Statistics and Applied probability 134, Published by CRC Press. Total number of pages: 18 + 462. ISBN: 978-1-4665-8322-1 (Hardback).
Killiches, M., Kraus, D., Czado C., 2017. Using model distances to investigate the simplifying assumption, model selection and truncation levels for vine copulas. Preprint.
Kysely, J., Gaal, L., Beranova, R., Plavcova, E., 2011. Climate change scenarios of precipitation extremes in Central Europe from ENSEMBLES regional climate models. Theor. Appl. Climatol. 104 (3–4), 529–542.
Kumar, P., 2010. Probability distributions and estimation of Ali-Mikhail-Haq Copula. Appl. Math. Sci. 4 (14), 657–666.
Ledford, A.W., Tawn, J.A., 1997. Modelling dependence within joint tail regions. J. R. Stat. Soc., Ser. B 59, 475–499.
Leonard, M., Westra, S., Phatak, A., Lambert, M., van den Hurk, B., McInnes, K., Risbey, J., Schuster, S., Jakob, D., Stafford-Smith, M., 2014. A compound event frame-work for understanding extreme impacts. Wiley Interdiscip. Rev.: Clim. Change 5 (1), 113–128.
Lewis, M., Bates, P., Horsburgh, K.J., Neal, J., Schumann, G., 2013. A storm surge inundation model of the northern Bay of Bengal using publicly available data. Q. J. R. Meteorol. Soc. 139, 358–369. https://doi.org/10.1002/qj.2040.
Li, B., Chen, Y., Shi, X., Chen, Z., Li, W., 2013. Temperature and precipitation changes in different environments in the arid region of northwest China. Theor. Appl. Climatol. 112 (3–4), 589–596.
Li, Q., Brown, J.B., Huang, H., Bickel, P.J., 2011. Measuring reproducibility of high-throughput experiments. Ann. Appl. Stat. 5.
Lian, J.J., Xu, K., Ma, C., 2013. Joint impact of rainfall and tidal level on flood risk in a coastal city with a complex river network: a case study of Fuzhou City, China. Hydrol. Earth Syst. Sci. 17 (2), 679–689. https://doi.org/10.5194/hess-17-679-2013.
Masina, M., Lamberti, A., Archetti, R., 2015. Coastal flooding: a copula based approach for estimating the joint probability of water levels and waves. Coastal Eng. 97, 37–52.
Müller, M., Kaspar, M., 2010. Quantitative aspect in circulation type classifications – an example based on evaluation of moisture flux anomalies. Phys. Chem. Earth 35, 484–490.
Nagler, T., Bumann, C., Czado, C., 2018. Model selection in sparse high-dimensional vine copula models. Department of Mathematics, Technische Universität München, Boltzmanstraße 3, 85748 Garching, Germany.
Nagler, T., Bumann, C., Czado, C., 2018. Model selection in sparse high-dimensional vine copula models. Department of Mathematics, Technische Universität München, Boltzmanstraße 3, 85748 Garching, Germany.
Papaioannou, G., Kohnová, S., Bacigál, T., Szolgay, J., Hlavčová, K., Loukas, A., 2016. Joint modelling of flood peaks and volumes: a copula application for the Danube River. J. Hydrol. Hydromechanics 64 (4), 382–392.
Pappadà, R., Durante, F., Salvadori, G., De Michele, C., 2017. Clustering of concurrent flood risks via Hazard Scenarios. Spatial Stat. https://doi.org/10.1016/j.spasta.2017.12.002.
Petroliagkis, T.I., Voukouvalas, E., Disperati, J., Bildot, J., 2016. Joint Probabilities of Storm Surge, Significant Wave Height and River Discharge Components of Coastal Flooding Events. EUR 27824 EN. https://doi.org/10.2788/677778.
Poulin, A., Huard, D., Favre, A.C., Pugin, S., 2007. Importance of tail dependence in bivariate frequency analysis. J. Hydrol. Eng. 12, 394–403. https://doi.org/10.1061/(asce)1084-0699(2007)12:4(394).
Pugh, D.T., 1987. In: Tides, Surges and Mean Sea-level: a Handbook for Engineers and Scientists. Wiley, Chichester, pp. 472.
Ramirez, J.A., Lichter, M., Coulthard, T.J., Skinner, C., 2016. Hyper-resolution mapping of regional storm surge and tide flooding: comparison of static and dynamic models. Nat. Hazards 1–20.
Ree, W.O., 1954. Handbook of channel design for soil and water conservation: Soil Conservation Service, U.S. Department of Agriculture, SCS-TP-61, 40 p.
RMSI, 2012. Morocco Natural Hazards Probabilistic Risk Analysis and National Strategy. Flood Hazard Report (Draft). Department of Economic and General Affairs, Kingdom of Morocco, World Bank.
Rouge, C., Ge, Y., Cai, X., 2013. Detecting gradual and abrupt changes in hydrological records. Adv. Water Resour. 53, 33–44. https://doi.org/10.1016/j.advwatres.2012.09.008.
Ryan, W.B.F., Carbotte, S.M., Coplan, J.O., O'Hara, S., Melkonian, A., Arko, R., Weissel, R.A., Ferrini, V., Goodwillie, A., Nitsche, F., Bonczkowski, J., Zemsky, R., 2009. Global Multi-Resolution Topography synthesis. Geochem. Geophys. Geosyst. 10, Q03014. https://doi.org/10.1029/2008GC002332.

Salvadori, G., 2004. Bivariate return periods via 2-copulas. Stat. Methodol. 1, 129–144.
Salvadori, G., De Michele, C., Kottegoda, N., Rosso, R., 2007. Extremes in Nature: An Approach Using Copulas, Water Sci. Technol. Libr., vol. 56. Springer, Dordrecht, Netherlands.
Samuels, P.G., Burt, N., 2002. A new joint probability appraisal of flood risk. Proc. Int. Civ. Eng. — Water Mar. Eng. 154 (2), 109–115.
Savu, C., Trede, M., 2010. Hierarchies of Archimedean copulas. Quant. Finance 10, 295–304. https://doi.org/10.1080/14697680902821733.
Sebastian, A., Dupuits, E.J.C., Morales-Nápoles, O., 2017. Applying a Bayesian network based on Gaussian copulas to model the hydraulic boundary conditions for hurricane flood risk analysis in a coastal watershed. Coastal Eng. 125, 42–50. https://doi.org/10.1016/j.coastaleng.2017.03.008.
Sheng, Y., Peter n.d., R., 2002. Bivariate frequency analysis: discussion of some useful concepts in hydrological application. Hydrol. Processes 16, 2881–2898. https://doi.org/10.1002/hyp.1185.
Silva, R.S., Lopes, H.F., 2008. Copula, marginal distributions and model selection: a Bayesian note. Stat Comput 18, 313. https://doi.org/10.1007/s11222-008-9058-y.
Skinner, C.J., Coulthard, T.J., Parsons, D.R., Ramirez, J.A., Mullen, L., Manson, S., 2015. Simulating tidal and storm surge hydraulics with a simple 2-D inertia-based model, in the Humber Estuary, UK Estuarine. Coastal Shelf Sci. 155, 126–136.
Sklar, M., 1959. Fonctions de répartition à n dimensions et leurs marges. Publications de l'Institut Statistique de Université de Paris 8.
Schmidt, R., Stadtmuller, U., 2006. Non-parametric estimation of tail dependence. Scand. J. Stat. 33 (2), 307–335.
Svensson, C., Jones, D.A., 2002. Dependence between extreme sea surge, river flow and precipitation in eastern Britain. Int. J. Climatol. 22 (10), 1149–1168.
Svensson, C., Jones, D.A., 2004. Dependence between extreme sea surge, river flow and precipitation in south and west Britain. Hydrol. Earth Syst. Sci. 8 (5), 973–992.
Schwarz, G., 1978. Estimating the dimension of a model. Ann. Stat. 6 (2), 461–464.
Van De Wiel, M.J., Coulthard, T.J., Macklin, M.G., Lewin, J., 2007. Embedding reach-scale fluvial dynamics within the CAESAR cellular automaton landscape evolution model. Geomorphology 90 (3–4), 283–301.
Van den Berg, M.J., Vandenberghe, S., De Baets, B., Verhoest, N.E.C., 2011. Hydrology and Earth System Sciences. Katlenburg-Lindau 15 (5), 1445.
Vose, D., 2010. Quantitative Risk Analysis. A Guide to Monte Carlo Simulation Modelling, 1st edition. John Wiley & Sons.
Wahl, T., Mudersbach, C., Jensen, J., 2012. Assessing the hydrodynamic boundary conditions for risk analyses in coastal areas: a multivariate statistical approach based on Copula functions. Nat. Hazards Earth Syst. Sci. 12, 495–510.
White, C.J., 2009. The use of joint probability analysis to predict flood frequency in estuaries and tidal rivers. PhD Thesis. University of Southampton School of Civil Engineering and the Environment.
Xiao, H., Lu, G.H., Wu, Z.Y., Liu, Z.Y., 2013. Flood response to climate change in the Pearl River 15 basin for the next three decades. J. Hydraul. Eng. 12, 1409–1419 (in Chinese).
Xu, K., Ma, C., Lian, J., Bin, L., 2014. Joint probability analysis of extreme precipitation and storm tide in a coastal city under changing environment. PLoS One 9 (10), e109341. https://doi.org/10.1371/journal.pone.0109341.
Yamazaki, D., Lee, H., Alsdorf, D.E., Dutra, E., Kim, H., Kanae, S., Oki, T., 2012. Analysis of the water level dynamics simulated by a global river model: a case study in the Amazon River. Water Resour. Res. 48, W09508. https://doi.org/10.1029/2012WR011869.
Zellou, B., Rahali, H., 2017. Assessment of reduced-complexity landscape evolution model suitability to adequately simulate flood events in complex flow conditions. Nat. Hazards 86, 1–29. https://doi.org/10.1007/s11069-016-2671-8.
Zhang, L., Singh, V.P., 2007. Bivariate rainfall frequency distributions using Archimedean copulas. J. Hydrol. 332, 93–109. https://doi.org/10.1016/j.jhydrol.2006.06.033.
Zheng, F., Westra, S., Sisson, S.A., 2013. Quantifying the dependence between extreme rainfall and storm surge in the coastal zone. J. Hydrol. 505, 172–187. https://doi.org/10.1016/j.jhydrol.2013.09.054.
Zheng, F., Westra, S., Leonard, M., Sisson, S.A., 2014. Modeling dependence between extreme rainfall and storm surge to estimate coastal flooding risk. Water Resour. Res. 50 (3), 2050–2071. https://doi.org/10.1002/2013WR014616.